NANOSCALE EFFECTS OF NICKEL CATIONS ON CALCITE GROWTH OBSERVED BY *IN SITU* ATOMIC FORCE MICROSCOPE

A Thesis

Presented to the Faculty of the Graduate School

of Cornell University

In Partial Fulfillment of the Requirements for the Degree of

Master of Science

by

Hengyu Zhou

December 2019

ABSTRACT

Biomineralization of calcite has been the focus of numerous studies, yet some intricate problems, especially those related to the mechanism of calcite-additive interactions remain poorly understood. Previous research has investigated how additives attach on the calcite growth steps and change step-edge properties of calcite hillocks. More recently, based upon both computational and experimental results, there is a growing interest in understanding what role the hydration layer on calcite plays in directing the interactions of additives. Nickel (II), an important micronutrient for organisms, has a solvation shell that is quite different from calcium. Such differences include the structure of the hydration shell, the enthalpy of solvation, and the hydrolysis kinetics. For these reasons, we chose to explore calcite growth in the presence of Ni cations to see how this cation disrupted the calcite hydration layer. Specifically, we used fluid cell AFM to monitor calcite growth in the presence of Ni^{2+}. We find that nickel cations have concentration-dependent effects on calcite hillock growth, including modification of hillock geometry, decrease in step density on both acute and obtuse sites, and increase in step velocities. Morphology of the growth hillocks is modified largely only when nickel chloride concentration is high enough (Ni:Ca ≈ 3% mol). After nickel is added, the step density on both acute and obtuse steps, as well as the height of a growth hillock keeps decreasing with time regardless of nickel concentration, until the hillock disappears from the surface, or the hillock reaches a steady state. Step velocities increase in every tested nickel concentration and most of them do not reach a steady state after a running time of ~2400 seconds. The acute step velocities always increase greatly (~200%) after nickel is added, while the obtuse step velocities first decrease and then start to increase. The faster step velocities are believed to result from modification of surface kinetics, which could indicate that the Ni^{2+} disrupts the hydration layer on the calcite surface,

making it easier for growth units to add to both acute and obtuse steps. These results provide insight into how small cations with large hydration shells can lead to unexpected changes to calcite growth kinetics, which may provide a route to modify the hydration layer on crystal surface and thus further influence the interaction between crystal and organic impurities.

BIOGRAPHICAL SKETCH

Hengyu Zhou was born in 1996 in Chengdu, China. He loved reading picture books about evolution in organisms since his childhood, which inevitably leads to a dream of becoming a scientist. In 2007, he was enrolled to Chengdu Foreign Languages School as a junior student at Science Experimental Class, a place where he first started to realize his dream. He learned fundamental science during the six years of junior high. He also built up his interests in popular science, mystery novels, and world history. His longing for freedom led him to study abroad, and his passion to explore drove him to study further in the field of art and science.

In 2013, he became an undergraduate student in Department of Mathematics at University of Illinois, Urbana-Champaign. After realizing his interest in material research and experimental practice, he transferred to Department of Materials Science of Engineering at the end of his sophomore year. He joined Professor Jian-Min Zuo's research group in his junior year and started his research career. He confirmed his interest in experimental studies on nanoscale characterization of materials and decided to pursue further in academics.

He was enrolled to Cornell University as a Master of Science student in Department of Materials Science and Engineering. He joined Professor Lara Estroff's research group after becoming inspired by the beautiful complexity in structures of biogenic crystals and biomaterials. After completing his Master of Science Degree, he will continue his studies in crystal growth at New York University for a doctorate degree in Department of Chemistry.

DEDICATIONS

To the ones I love from all worlds and dimensions

ACKNOWLEDGMENTS

My current achievements in this work would be impossible without everyone I met at Cornell, who supported me in my academic, research, and daily life. Though I dislike the cold weather in Ithaca, Cornell University, especially the Estroff Lab at SB60 of Bard Hall, has always been a warm home for me. I enjoyed my time at Cornell a lot and it is always my greatest pride to be a Cornellian.

I would first thank my advisor, Professor Lara Estroff, for her patient instructions, inspiring thoughts and insightful ideas which always encouraged me in the past two years. She has provided me with the best support I could have ever asked for.

Then I would like to thank everyone in the Estroff group for their advice and help during the past two years. Specially, I would like to thank Amnon Ortoll-Bloch for teaching me on the device and giving me thoughtful suggestions on my experimental setup. I would also like to thank Damian Palin, Abby Goldman, Jennie Kunitake, Reum Scott and Konrad Hendrick for their instructions on lab instruments, suggestions on my experimental practice, help on my group jobs, and support on my thesis writing and presentation.

In addition, I would like to thank Professor Shefford Baker for being my committee member and providing me with helpful feedbacks on during several of our meetings in the past two years. I would also like to thank Professor Lena Kourkoutis and Professor Itai Cohen for their insightful advice on my project and great instructions on my presentation skills. I would like to specially thank Dana Chapman, and Fei Yu from the Wiesner group, for helping me on getting fresh de-ionized water.

I got great support from out of my institution as well. I thank Dr. Jinhui Tao from Pacific Northwest National Laboratory for his insightful comments on my experimental results. I would

also like to thank Dr. Jim De Yoreo, Dr. Christine Orme, Dr. Jeffery Rimer and Dr. Rosa Espinosa-Marzal for their helpful advice on my work during their visits to Cornell. I would like to thank every professor and graduate student I met during Gordon Research Conference: Biomineralization 2018 for their comments on my project.

Many thanks to Hao Zhou and Jiaxin Sun for being my excellent roommates, especially for recognizing me as a big eater, making extra food when they cook and sharing the delicious food with me even if I am on a diet.

Finally, I sincerely thank my family for their trust in me, their financial support during my past 6 years of studying abroad, and most importantly, their love for me throughout my life.

TABLE OF CONTENTS

LIST OF FIGURES

and "-" signs corresponds to obtuse and acute steps respectively. (a) reprinted from ref.9 with permission from ACS copyright 2008. (b) reprinted from ref.10 with permission from Springer copyright 2013. (c) reprinted from ref.11 with permission from SPSJ copyright 2015. (d) reprinted from ref.12 with permission from Elsevier copyright 1998.

Diagrams showing how AFM works: (a) Diagram illustrating basic components of an AFM, including a cantilever, a laser source and a photodetector. (b) Diagram showing how tip scans across a surface and integrate each scan to a complete image. (c) A typical AFM image of a growing calcite hillock. Features including the peak, steps, obtuse and acute regions marked by "+" and "-" signs, and even surface defects are revealed under AFM. (a,b) reprinted from ref.6 with permission from RSC copyright 2012.

In situ AFM studies conducted on Mg-Ca system. (a-c) AFM images of calcite hillock growth. Comparison between (a) and (b) shows a decrease in step velocity with decreasing calcite supersaturation. Geometry change as well as step velocity decreasing from (b) to (c) indicates the influence of Mg^{2+} on calcite growth. (a-c) reprinted from ref.5 with permission from MRS copyright 2000.

AFM image of a calcite hillock on (104) facet. The left image shows hillock growth at σ=0.3 and the right image shows hillock growth at σ=0.8. Larger supersaturation causes obvious increase in step density. Figure reprinted from ref.19 with permission from Elsevier copyright 2000.

In situ AFM images of control experiments done on calcite growth with Mg^{2+} in different IS values, indicating change of IS also severely influence calcite growth. (a) IS=0.1M KCl, without Mg^{2+}. (b) IS=0.1M KCl, $a_{Mg^{2+}}/a_{Ca^{2+}} = 1/4$.(c) IS=0.1M KCl, $a_{Mg^{2+}}/a_{Ca^{2+}} = 1/3$. (d) IS=0.1M NaCl, $a_{Mg^{2+}}/a_{Ca^{2+}} = 1/3$. (a-d) adapted and reprinted from ref.15 with permission from Elsevier copyright 2011.

(a-c) A representative set of AFM images of calcite hillocks growing with highly anionic $PMAA_{85}$-$PBzMA_{100}$ nanoparticles. The particles can be visualized on the surface and are affecting hillock geometry to a large extent. (d) A representative SEM image of bulk calcite grown in the presence of $PMAA_{85}$-$PBzMA_{100}$ nanoparticles. The calcium concentration in growth solution is 5mM with a copolymer concentration of 0.75 wt%. (e) Schematic diagrams showing the interaction between the hydration layer and the micelle charged corona. Small dots represent ion distribution on calcite surface. The two images compare conditions under different supersaturation and IS. (a-d) adapted and reprinted from ref.20 with permission from ACS copyright 2018. (e) reprinted from ref.21 with permission from license of Attribution 4.0 International.

LIST OF ABBREVIATIONS

AFM	Atomic Force Microscope
$CaCO_3$	Calcium Carbonate
$CaCl_2$	Calcium Chloride
ICP	Inductively Coupled Plasma
$(NH_4)_2CO_3$	Ammonium Carbonate
NaCl	Sodium Chloride
$NaHCO_3$	Sodium Bicarbonate
$NiCl_2$	Nickel Chloride
$NiCO_3$	Nickel carbonate
SEM	Scanning Electron Microscope

CHAPTER 1

IN SITU ATOMIC FORCE MISCROSCOPY STUDIES ON CRYSTAL-ADDITIVE INTERACTION MECHANISMS IN CALCITE SYSTEMS

Abstract

The beautiful complexity of crystal growth in natural calcite systems provides researchers with valuable prospects for developing functional and structural materials. To better design and synthesize bio-inspired materials, understanding the mechanism of calcite growth is essential. Visual observation of nanoscale details of calcite growth, using techniques such as *in situ* atomic force microscopy (AFM), offers unique insight into the surface properties of growing crystals. In this chapter, I review *in situ* AFM studies on calcite growth with additives. Specifically, I present mechanisms of calcite growth and a brief introduction to the technique of in *situ* AFM characterization. I review the status quo of *in situ* AFM studies conducted on calcite growth with additives and introduce gaps in current knowledge. Finally, I propose an experimental design to increase our understanding of calcite-additive interaction mechanisms, with a focus on the surface chemistry during calcite growth.

1.1 Motivation

An astonishing diversity of morphologies of calcite crystals are produced by a wide range of organisms [1]. The biogenic calcite crystals in these systems usually have higher hardnesses and toughnesses as compared to geologic calcite and excellent adaptivity in various environments[2,3]. As people are trying to mimic these bio-systems to design advanced materials and synthesize crystals with desired nanostructures, understanding the mechanism of calcite crystallization becomes the first priority[1–3]. While supersaturation and growth mechanism have dominating effects on crystal habits in abiotic solution growth, the wide variety of forms shown in these organisms (see Fig. 1.1) also imply that subtle changes in physical and chemical conditions are key factors in biogenic crystallization[1,4]. Specifically, impurities such as other inorganic anions and biomacromolecules are implicated as key factors that affect the crystallization process in biology[4,5].

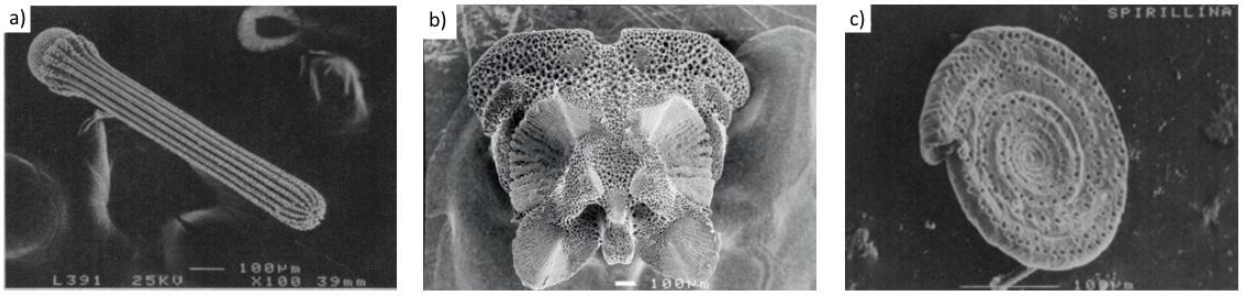

Fig. 1.1 Scanning electron microscope images of different kind of natural single crystal calcites. (a) A newly formed spine of sea urchin found in eastern Mediterranean. The axis of this spine is parallel to the crystallographic *c* axis of calcite. (b) A vertebra in an arm of a brittle star. Though its morphology is convoluted, this vertebra consists of only two calcite single crystals joined along the vertical plane of symmetry. (c) Shell of the foraminifera *Spirillina*, which also consists of a single crystal calcite. (a,c) reprinted from ref.4 with permission from AAAS copyright 1993. (b) adapted and reprinted from ref.1 with permission from IOP copyright 2014.

In early research, scientists characterized calcite crystals, *ex situ*, using scanning electron microscope (SEM) and realized that it was impossible to understand crystal-additive mechanisms without directly visualizing the whole process of crystal growth[1,4]. The urgent need for *in situ*

characterization is satisfied by the advancement of atomic force microscopy (AFM) in liquid and its capability to observe a constantly changing surface. Three advantages of AFM have made this technique one of the most promising and widely applied technique for *in situ* characterization of crystal growth[6]. Firstly, AFM can directly visualize a crystallization event without disrupting the crystallization process or causing damage to the sample. Secondly, the high resolution of AFM images facilitates direct characterization of crystal-additive interaction process. AFM is proven to provide extremely high vertical resolution as well as lateral resolution. A study on tetracene growth presents the high resolution of a typical AFM (Fig. 1.2)[7]. In this study, tetracene platelets characterized under AFM have a height of only 10 to 15 unit cell lengths, indicating the excellent ability of AFM in vertical detection. Another higher magnification image shows the exceptional lateral resolution of AFM, where fine surface structures are revealed (Fig. 1.2c). Such high-resolution characterization is perfect for *in situ* crystal growth characterization, where we aim to visualize how crystal growth is altered in the presence of additives. Thirdly, the AFM is an

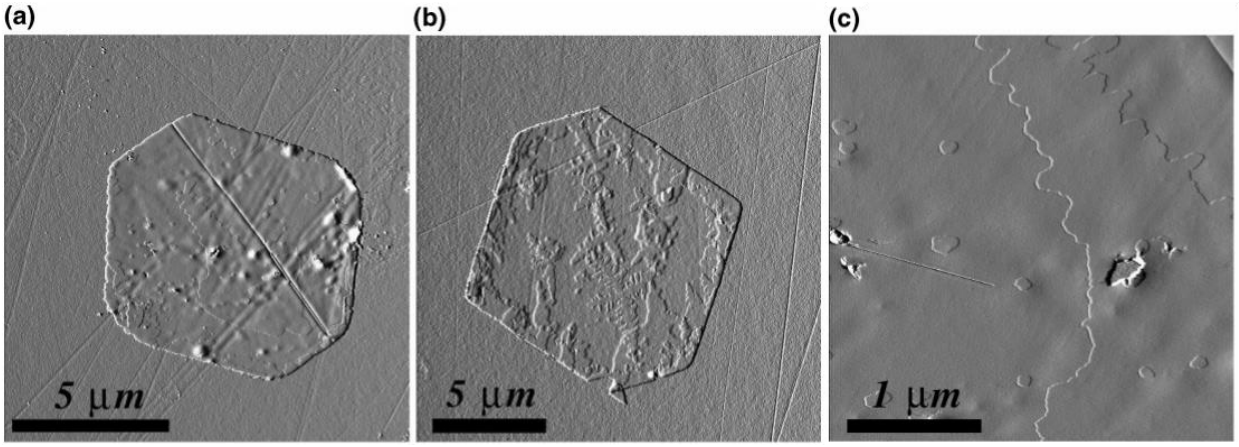

Fig. 1.2 Atomic force microscope (AFM) images of a tetracene growth surface. (a) (b) AFM images of tetracene islands. The AFM shows excellent height contrast of only 10 to 15 unit cell lengths, showing high vertical resolution of this technique. (c) A zoomed-in AFM image showing fine structures on tetracene surface. Details of a few nanometers are revealed under AFM, showing its high resolution in lateral space. (a-c) reprinted from ref.7 with permission from ACS copyright 2004.

affordable technique to researchers, since the laboratory prerequisites for installing and operating AFM is much simpler than any similar device such as electron microscopes. AFM can operate without complicated sample preparation, high vacuum or strictly controlled temperature. Thus, AFM has become a widely used technique for *in situ* studies on crystal growth.

1.2 Background: calcite growth model characterized by AFM

When a calcite surface is exposed to a supersaturated environment, heterogeneous calcite growth begins[8]. Based on previous research, heterogeneous calcite growth follows the Terrace-Step-Kink (TSK) model (Fig. 1.3a)[8,9]. This model simplifies growth units as cubes, divides a crystal surface into terraces (one available surface for forming bonds), steps (two available surfaces for forming bonds), and kinks (three available surfaces for forming bonds). Near-equilibrium, kink sites can form more bonds with growth units, making it energetically favorable for attachment events. On a flat surface, a surface screw dislocation is a natural kink site for growth units to attach on, which becomes the source of calcite spiral hillock growth (Fig. 1.3b)[10]. According to the molecular structure of calcite, the steps formed can be characterized as acute steps and obtuse steps, the difference between which is an important factor affecting attachment

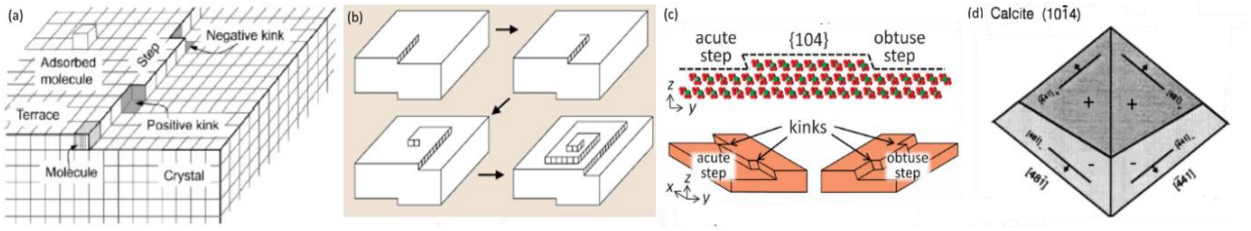

Fig. 1.3 Illustration of heterogeneous calcite growth: (a) Schematic drawing of the TSK model showing terrace, step and kink features of a crystal surface. (b) Schematic diagram of spiral growth taking place from a natural screw dislocation. (c) Schematic diagram of acute and obtuse steps for a calcite {104} facet. (d) Schematic diagram showing four vicinal faces on a calcite (104) face. "+" and "-" signs corresponds to obtuse and acute steps respectively. (a) reprinted from ref.9 with permission from ACS copyright 2008. (b) reprinted from ref.10 with permission from Springer copyright 2013. (c) reprinted from ref.11 with permission from SPSJ copyright 2015. (d) reprinted from ref.12 with permission from Elsevier copyright 1998.

of growth units in the presence of additives (Fig. 1.3c)[11]. Taking a typical calcite {104} face as example, a calcite hillock has four vicinal faces with two acute steps labeled with "-" and two obtuse steps labeled with "+" (Fig. 1.3d)[12].

AFM can reveal processes of calcite hillock growth in aqueous solution[6]. AFM is a photon-based device built upon a cantilever, a laser, and a detector. A laser source shoots at the head of the cantilever and reflects to a certain position on the detector. Attached to the cantilever head is a tip whose width is usually less than 5 nm. The cantilever deflects at different surface features due to the repelling force between the surface and the tip. The laser reflection position is thus changed according to motion of the cantilever and the detector collects these tiny changes (Fig. 1.4a). Lock-in amplifiers enhance these signals and convert them to images with height profiles [6]. The tip normally does linear scans and rasters across a surface to form a complete image (Fig. 1.4b)[6]. A typical AFM image of a calcite growth hillock shows clear features including the peak, steps as well as obtuse and acute regions (Fig. 1.4c).

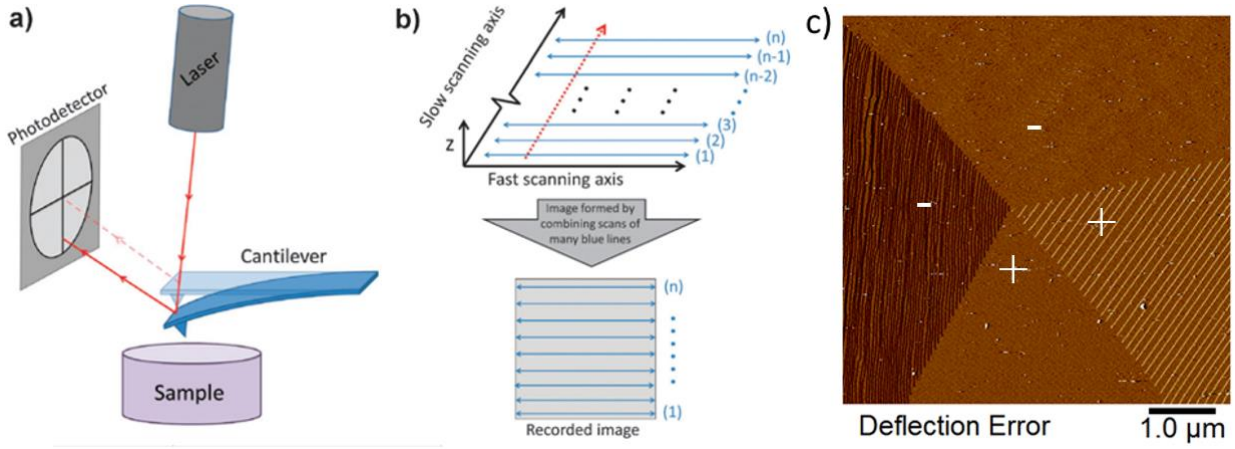

Fig. 1.4 Diagrams showing how AFM works: (a) Diagram illustrating basic components of an AFM, including a cantilever, a laser source and a photodetector. (b) Diagram showing how tip scans across a surface and integrate each scan to a complete image. (c) A typical AFM image of a growing calcite hillock. Features including the peak, steps, obtuse and acute regions marked by "+" and "-" signs, and even surface defects are revealed under AFM. (a,b) reprinted from ref.6 with permission from RSC copyright 2012.

1.3 AFM studies of additive interactions with calcite

The presence of cations, other than Ca, in calcite growth solutions affect crystallization in various aspects. Divalent cations, due to their charge similarity to calcium ions, are typical impurities that modify growth mechanisms greatly. One of the most studied divalent cations in calcite growth is magnesium (Mg^{2+}). The ubiquity of Mg^{2+} in natural water makes it the principal modifier of calcium carbonate morphology and its growth mechanism in biogeochemical environments[13]. The De Yoreo group has conducted a series of *in situ* AFM experiments on Ca-Mg system[5,14,15]. In earlier studies, the De Yoreo group mainly focused on step velocity studies revealing incorporation effect of Mg^{2+} on calcite growth (Fig. 1.5a-c)[5]. Observations by *in situ* AFM clearly demonstrate how Mg^{2+} additives modify calcite growth hillocks. The shape of calcite hillocks changes in the presence of Mg^{2+} additives, and quantitative analysis on step migration rates indicates that the step velocity linearly decreases as a function of Mg^{2+} concentration. Such reduction in step velocity satisfies Qiu's incorporation mechanism[9], where Mg^{2+} substitutes for Ca^{2+} in the calcite lattice and induces lattice strain, leading to inhibition of step growth. Later this group has conducted a follow-up research on how magnesium incorporates into calcite hillocks[14]. By studying step velocities at various directions, they have found that the step velocity changes differently corresponding to different directions. Mg^{2+} preferentially inhibits step growth at the boundary between acute (-) and obtuse (+) edges and Mg^{2+} incorporation favors acute steps more than obtuse steps. This experimental result indicates that Mg^{2+} has a preference when incorporating on step edges and can cause calcite morphology transition simply by altering the orientation of steps.

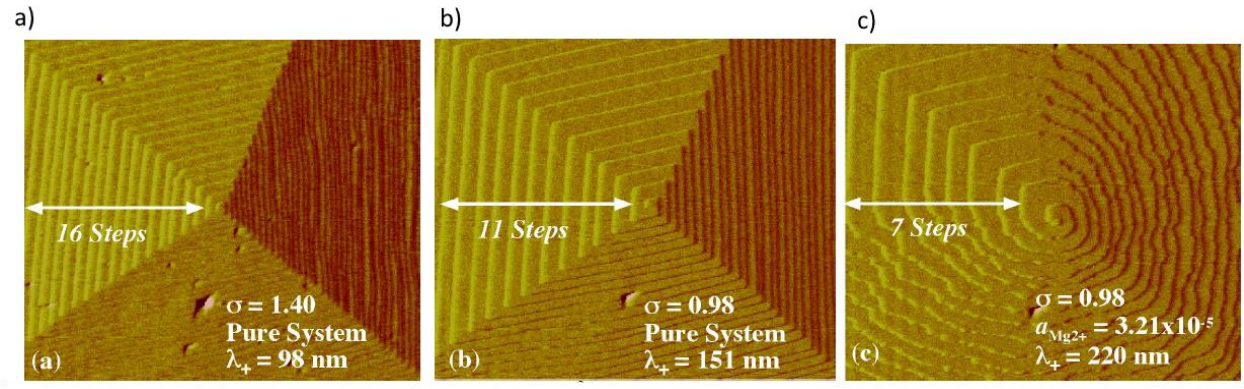

Fig. 1.5 In situ AFM studies conducted on Mg-Ca system. (a-c) AFM images of calcite hillock growth. Comparison between (a) and (b) shows a decrease in step velocity with decreasing calcite supersaturation. Geometry change as well as step velocity decreasing from (b) to (c) indicates the influence of Mg^{2+} on calcite growth. (a-c) reprinted from ref.5 with permission from MRS copyright 2000.

Scientists have also studied cations with various charge properties, such as selenium. In a recent study[16], researchers found that Se(IV), Se(VI) and Se(-II) affect calcite growth in different ways. Incorporation of Se(IV) to calcite surface was observed using *in situ* AFM and such incorporation behavior heavily modified hillock morphology (Fig. 1.6b). Further study indicated that 80% of Se(IV) from the solution was incorporated to calcite crystals. In comparison, Se(VI) did not incorporate but instead promoted step propagation rate without changing the growth pattern. Se(-II) applied in this study was in the form of seleno-L-cystine. This organic selenium influenced nucleation of calcite crystals observed under transmission electron microscope, while it had no obvious influence on geometry of calcite hillocks.

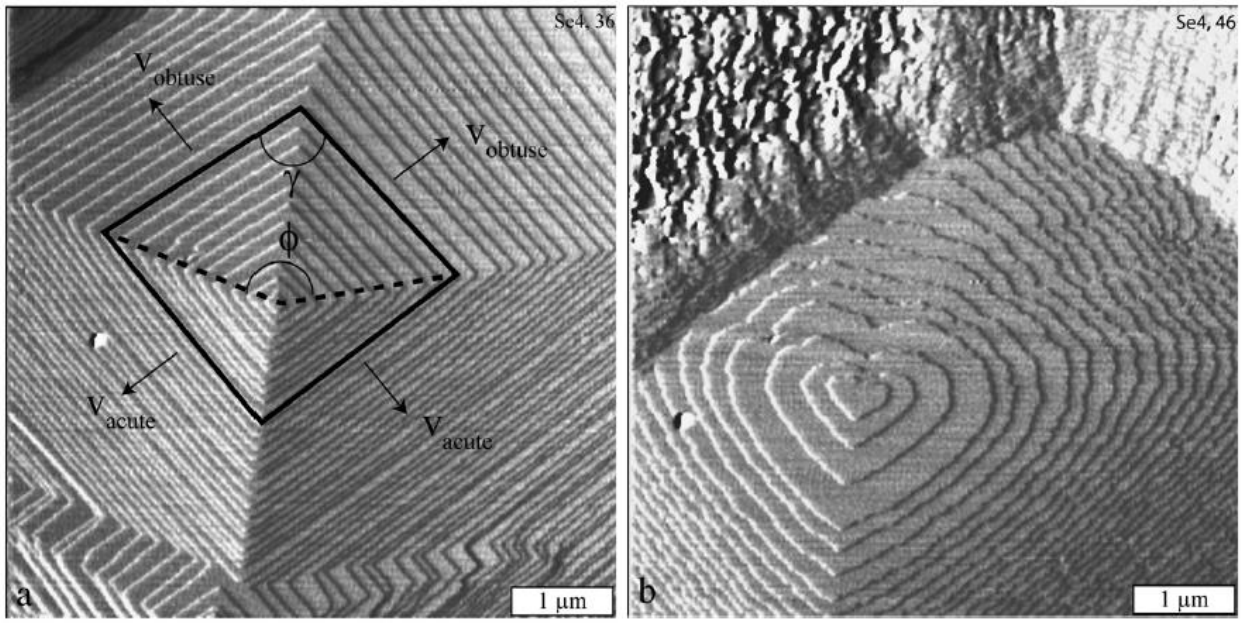

Fig. 1.6 In situ AFM studies conducted on Se(IV)-Ca system. (a) an AFM image of a calcite hillock growing from pure calcite growth solution. (b) an AFM image of the same hillock after the addition of Se(IV). The steps were rounded and the morphology of the hillock was modified into a heart shape. (a, b) reprinted from ref.16 with permission from Elsevier copyright 2013.

Besides ionic additives, researchers have also applied AFM to study organic growth modifiers in calcite systems, where the interaction mechanism can be more complicated. Orme et al. have studied chiral morphologies of calcite with L-Aspartic acid and D-aspartic acid inclusions[17]. *In situ* AFM experiments reveal that the geometry of calcite hillocks changes significantly with the presence of amino acids while calcite hillocks in the prescence of the two chiral additives grow as mirror images of each other (Fig. 1.7a-b). Such AFM discovery is consistent with *ex situ* SEM observation where the calcite crystals grown with L-Asp and D-Asp are also mirror images of each other (Fig. 1.7c-d). Besides the modification on hillock morphology, the amino acids also showed a trend to attach on the acute steps of the calcite hillock. Calcite growth with chiral additives indicates that L-Asp and D-Asp bind to the calcite in

different ways according to their chiral structures, changing the surface free energy of calcite hillocks and inducing formation of chiral calcite crystals accordingly[17].

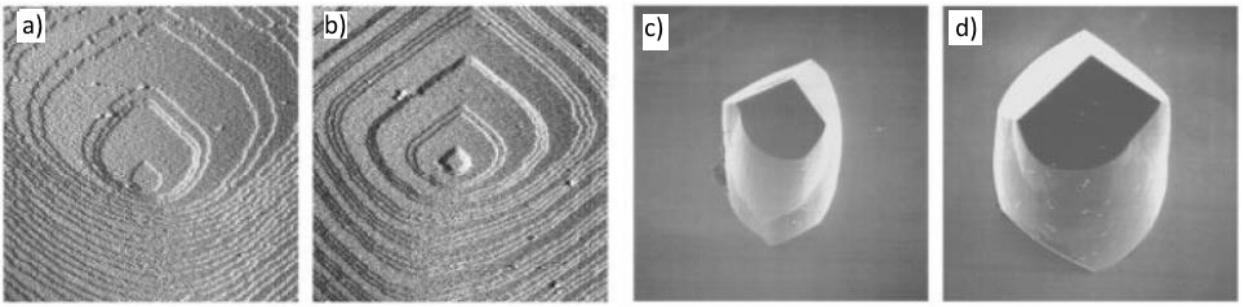

Fig. 1.7 *In situ* AFM studies on calcite with chiral amino acids. (a-b) AFM images of calcite hillocks growing with L-Asp (a) and D-Asp (b). The hillock geometry is mirror image of each other. (c-d) SEM images of ex situ grown calcite with L-Asp (c) and D-Asp (d). The results are consistent with AFM observations. (a-d) adapted and reprinted from ref.17 with permission from Macmillan Magazines copyright 2001.

1.4 Indication of interaction mechanisms: step velocity and hillock geometry

1.4.1 Step velocity analysis

The growth rate of a crystal via attachment of growth units can be analyzed by measuring hillock step velocity[18]. In calcite, the step velocities are different for obtuse and acute steps and these velocities can be expressed by the equation:

$$v = \beta\omega(a_{Ca^{2+}} - a_{Ca^{2+}{}_{eq}}) \qquad \text{(eq. 1.1)}$$

where v is the step velocity, β is the kinetic coefficient, ω is the molecular volume of calcite, $a_{Ca^{2+}}$ is the activity of calcium cations, and $a_{Ca^{2+}{}_{eq}}$ is the activity of calcium cations at equilibrium. $a_{Ca^{2+}} - a_{Ca^{2+}{}_{eq}}$ indicates effective supersaturation, which is the actual supersaturation under which the spiral hillock growth is happening. For calcite, ω does not change while the presence of impurities may modify β and $a_{Ca^{2+}} - a_{Ca^{2+}{}_{eq}}$.

By quantitatively characterizing step velocity of the calcite hillocks using *in situ* AFM, Qiu et al. proposed four different mechanisms of crystal-additive interactions, providing a general classification of growth behaviors broadly applicable for hillock-dominated crystal growth (Fig. 1.8)[9]. The first mechanism is incorporation of additives, where the impurity ions substitute calcium ions and cause strain on the liquid-solid interface. Equilibrium solubility of calcite is changed and thus the step velocity curve shifts over without changes in the shape or slope of the curve (Fig. 1.8a). The second mechanism is the change of kinetic coefficient β caused by the presence of additives. Such a change in kinetic coefficient can either increase or decrease the slope of the velocity curve (Fig. 1.8b). The additives can also adsorb to the growing edges and block the motion of steps. The pinning of additives to the steps thus form some particular areas where the step velocity is much slower compared to other regions. Step growth can overcome the pinned additives after a certain growth time due to high local potentials, thus the step velocity curve converges eventually (Fig. 1.8c). In the last mechanism, additives act as surfactants which change the surface free energy γ, causing an alteration of hillock geometry (Fig. 1.8d).

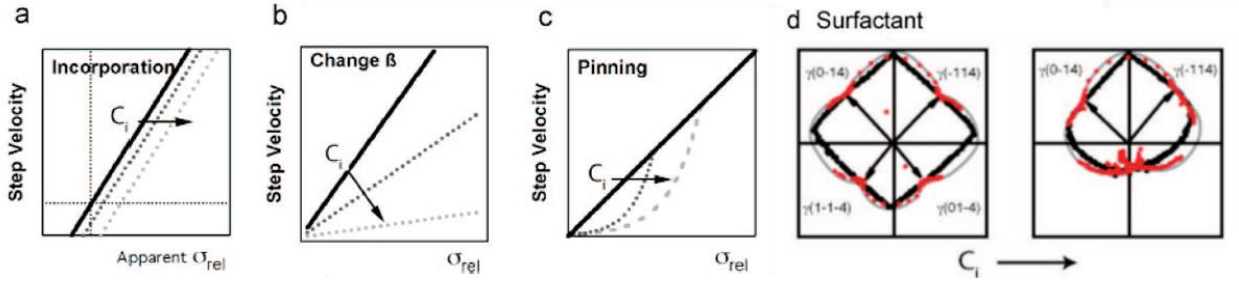

Fig. 1.8 Step velocity plots (a~c) and γ plots (d) elaborate different additive-crystal interaction mechanisms. In the first three mechanisms, additives change the step velocity either by inducing physical strain to the steps (a and c) or by changing the step-edge kinetic coefficient (b). In the last mechanism (d), the additives affect surface free energy of the hillock and shift the growth equilibrium to a particular orientation. As concentration of additives increase, the growth rate for bottom edges changes significantly and the hillock shifts to the top. (a-d) reprinted from ref.9 with permission from ACS 2008

1.4.2 Hillock geometry analysis

Hillock geometry is an important indication of crystal-additive interaction mechanisms. since even trivial disruption on both surface thermodynamics and kinetics can result in observable changes on hillock geometry. Hillock geometry can be characterized by hillock morphology and step density.

After the addition of impurities, whether hillock morphology is modified can be directly observed under AFM. Incorporation and step-pinning behaviors usually cause obvious change in hillock morphology in calcite. In these two mechanisms, the impurities compete with calcium (or carbonate) ions at certain sites such as step edges and kink sites. Incorporation of the structurally different ions or molecules induces strain, modifying hillock morphology. Pinning of the growth steps causes rounding effects on step edges, since the step growth does not have large enough driving force to grow through the pinning sites. Surfactants, including some organic molecules, can modify hillock morphology more easily and obviously by changing the surface free energy, which eventually results in a shift of preferred attachment site on calcite hillocks.

Since modification of hillock morphology by additives is the most straightforward effect to visualize using AFM, it provides us with readily obtainable information about interaction mechanisms. For example, we can judge whether the acute steps or the obtuse steps are more likely being affected by inclusion of additives. We can also predict the rounding of certain facets in bulk crystals by observing shift in hillock morphology under AFM.

Modification in hillock morphology usually involves a change in step density. However, the additives sometimes can change step density without modification of hillock morphology. Instead, the additives only modify the step density, which can be interpreted as steps per unit distance, or hillock slope. Typically, step density is an indication of how robustly the hillock is

growing. The density increases as effective supersaturation $a_{Ca^{2+}} - a_{Ca^{2+}eq}$ increases. Such an increment can be achieved by increasing supersaturation of calcium in the solution[19] (Fig.1.9), or by decreasing the equilibrium supersaturation. When the supersaturation is kept unchanged, change in step density indicates that the additives affect surface thermodynamics, changing the equilibrium supersaturation, and thus causing changes to hillock step density.

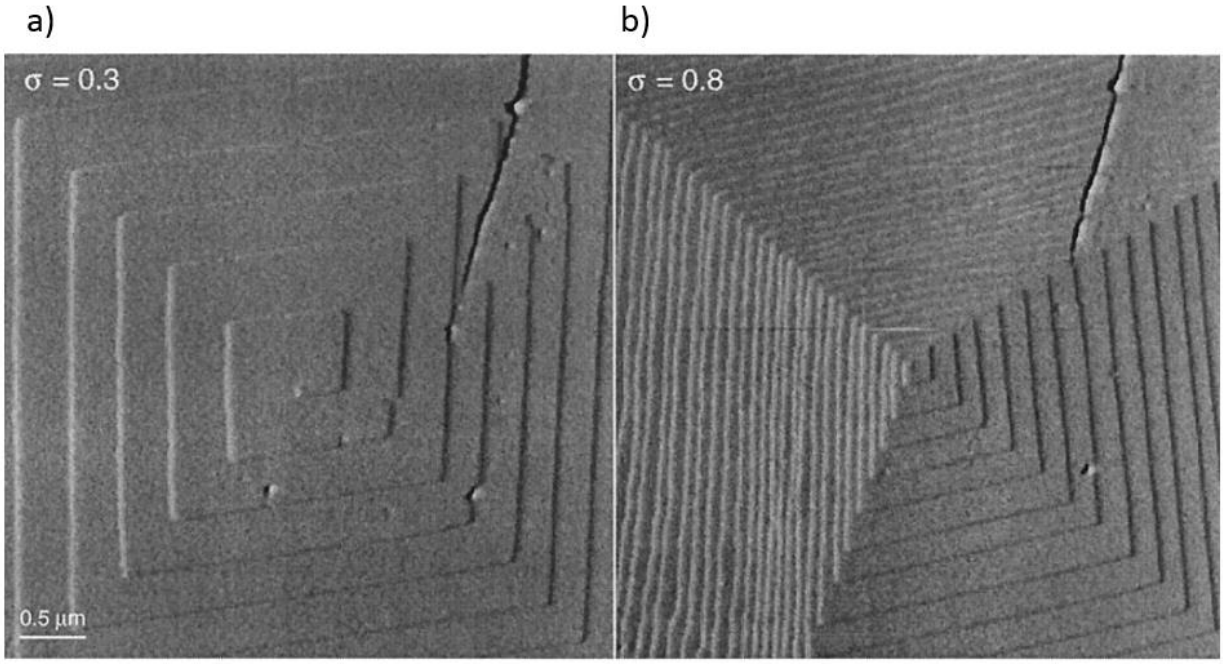

Fig. 1.9 AFM images of a calcite hillock on (104) facet, (a) hillock growth at σ=0.3 (b) hillock growth at σ=0.8. Larger supersaturation causes obvious increase in step density. Figure reprinted from ref.19 with permission from Elsevier copyright 2000.

1.5 Recent research: a shift of focus and new challenges

Previous research has focused on how additives incorporate to the calcite surface and change step-edge properties of calcite hillocks. People have realized that the classical models overlooked the chemical path by which the additives change the surface properties of crystals, for example, how they interact with hydration layers. More recent studies have focused on filling

these knowledge gaps by using *in situ* techniques to study how additives alter the calcite surface chemistry and the calcite-water interface.

In a follow-up research on the Ca-Mg system, the De Yoreo group has focused on the effect of ionic strength (IS) on calcite growth[15]. The AFM observations reveal different hillock structures with presence of magnesium as well as KCl and NaCl electrolytes of various solute activity values (*a*) (Fig. 1.10). As the IS value changes, the angle between acute-obtuse boundaries also changes to a large extent, forming completely different hillock geometry (Fig. 1.10 c-d). The results imply that an increase in ionic strength suppresses the uptake of Mg into calcite. Based on this conclusion, ionic strength in the growth solution may be considered as another critical factor that affects calcite crystallization.

Although this study provides insight into a chemical aspect of calcite-additive interactions, it failed to explain the fact that other studies report a positive correlation between Mg uptake and ionic strength[15]. Such conflict between reported results emphasized current knowledge gaps and reminds us of the importance to understand predominant mineralization

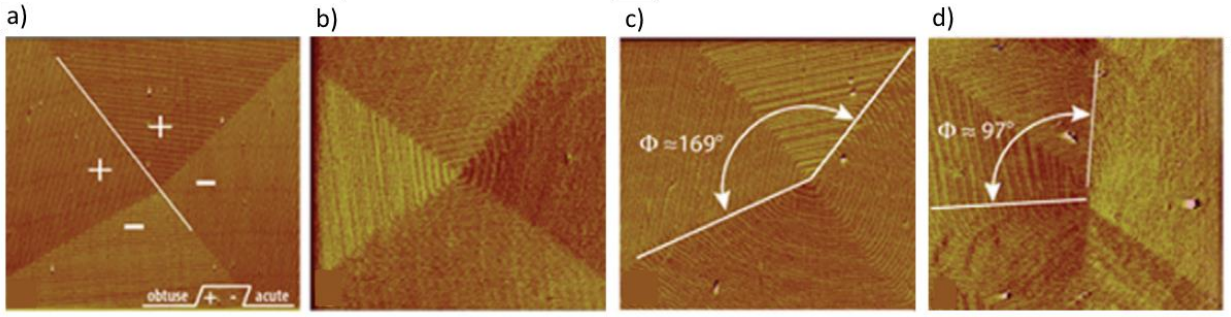

Fig. 1.10 *In situ* AFM images of control experiments done on calcite growth with Mg^{2+} in different IS values, indicating change of IS also severely influence calcite growth. (a) IS=0.1M KCl, without Mg^{2+}. (b) IS=0.1M KCl, $a_{Mg^{2+}}/a_{Ca^{2+}} = 1/4$.(c) IS=0.1M KCl, $a_{Mg^{2+}}/a_{Ca^{2+}} = 1/3$. (d) IS=0.1M NaCl, $a_{Mg^{2+}}/a_{Ca^{2+}} = 1/3$. (a-d) adapted and reprinted from ref.15 with permission from Elsevier copyright 2011.

process, such as the transformation of amorphous precursors to calcite, and the attachment process of calcium and carbonate ions onto the substrate through the hydration layer.

Another study done by Hendley et al. reveals the interaction mechanisms between diblock-copolymers and calcite[20,21]. A representative set of AFM images shown in Fig. 9 demonstrates geometry change of calcite hillocks by adding anionic poly(methacrylic acid)-stabilized poly(benzyl methacrylate) nanoparticles ($PMAA_{85}$-$PBzMA_{100}$), which forms a micelle structure surrounded by anionic charged corona in aqueous solution . Both step velocity and shape of hillock change significantly after the addition of micelles and the micelles attached on calcite surface can be directly observed (pointed out by yellow arrows in Fig.1.11c). By analyzing micelle motions observed under AFM, Hendley et al. have concluded three mechanisms that micelles can attach to calcite surface. The micelles may incorporate to the surface, which is similar to the interaction between calcite and magnesium cations. The micelles may also hover on the surface without becoming incorporated. Furthermore, the micelles can detach from the calcite surface after attaching on it, leaving an empty site on the surface[20,21].

This study gives mechanistic insight into interactions between organic particles and calcite surface, especially in the aspect of possible disruption of the calcite hydration layer induced by the large organic particles. Although the proposed mechanisms of micelle-calcite interaction have solid experimental evidence, the reason why the micelles interact with calcite surface in such manners remains unknown. In addition, even though we learned from this study that the interaction between micelles and calcite is determined by local electrochemical environment, we still do not know how the calcite hydration layer affects attachment of organic

particles. Problems raised in recent researches remain unsolved, and it is necessary to conduct more detailed studies on understanding the predominant mineralization process.

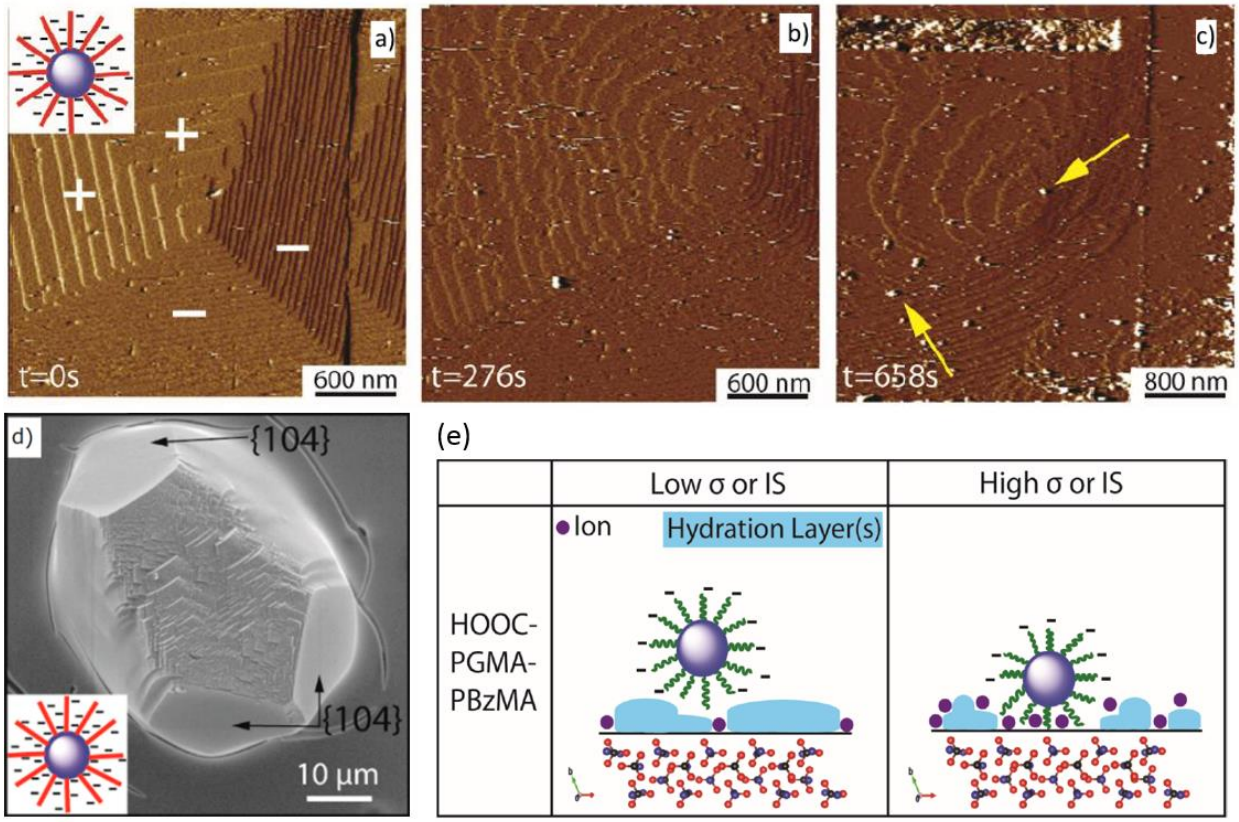

Fig. 1.11 (a-c) A representative set of AFM images of calcite hillocks growing with highly anionic $PMAA_{85}$-$PBzMA_{100}$ nanoparticles. The particles can be visualized on the surface and are affecting hillock geometry to a large extent. (d) A representative SEM image of bulk calcite grown in the presence of $PMAA_{85}$-$PBzMA_{100}$ nanoparticles. The calcium concentration in growth solution is 5mM with a copolymer concentration of 0.75 wt%. (e) Schematic diagrams showing the interaction between the hydration layer and the micelle charged corona. Small dots represent ion distribution on calcite surface. The two images compare conditions under different supersaturation and IS. (a-d) adapted and reprinted from ref.20 with permission from ACS copyright 2018. (e) reprinted from ref.21 with permission from license of Attribution 4.0 International.

1.6 Conclusion

As reviewed in this chapter, we have learned that while previous research has investigated how additives physically incorporate to the calcite surface and change step-edge properties of calcite hillocks, recent studies have started to focus on chemical driving forces affecting calcite hillock growth, such as ionic strength of the environment and surface chemistry of calcite hydration layer. Particularly in the work of Hendley et al., *in situ* AFM studies have revealed different mechanisms of the attachment of large organic molecules to the calcite surface and provided inspiring results on micelle-calcite interaction. However, it remains unclear as to how the calcite hydration layer influence the incorporation of these organic additives into calcite. With recent advances in techniques, researchers are able to directly characterize hydration layer on calcite surface[22–24], which further raises our interest on how impurities interact with the hydration layer on calcite surface.

In this thesis work, I propose an approach to better understand how the calcite hydration layer influence attachment of calcite growth units on calcite surface. I studied calcite growth in the presence of nickel additives and observed changes in hillock growth by *in situ* AFM. Though we do not directly visualize the hydration layer, our preliminary yet vital results can provide promising insight on how divalent cations with large hydration shells disrupt crystal surface hydration structure and how such disruption affect crystallization process.

1.7 Reference

1. Addadi, L. & Weiner, S. Biomineralization: Mineral formation by organisms. *Phys. Scr.* **89**, (2014).
2. Ma, Y., Weiner, S. & Addadi, L. Mineral deposition and crystal growth in the continuously forming teeth of sea urchins. *Adv. Funct. Mater.* **17**, 2693–2700 (2007).
3. Aizenberg, J. & Hendler, G. Designing efficient microlens arrays: Lessons from Nature. *J. Mater. Chem.* **14**, 2066–2072 (2004).
4. Berman, A. *et al.* Biological control of crystal texture: A widespread strategy for adapting crystal properties to function. *Science (80-.).* **259**, 776–779 (1993).
5. Davis, K. J., Dove, P. M. & De Yoreo, J. J. Resolving the Control of Magnesium on Calcite Growth: Thermodynamic and Kinetic Consequences of Impurity Incorporation for Biominernal Formation. *Mat. Res. Soc. Symp.* **620**, 1–7 (2000).
6. Chow, E. H. H., Bučar, D. K. & Jones, W. New opportunities in crystal engineering - The role of atomic force microscopy in studies of molecular crystals. *Chem. Commun.* **48**, 9210–9226 (2012).
7. Cuppen, H. M., Graswinckel, W. S. & Meekes, H. Screw dislocations on polycenes: A requirement for crystallization. *Cryst. Growth Des.* **4**, 1351–1357 (2004).
8. Roger, R. J. & Garside, J. From molecules to crystallizers. ISBN: 9780198504894 (2000).
9. Qiu, S. R. & Orme, C. A. Dynamics of biomineral formation at the near-molecular level. *Chem. Rev.* **108**, 4784–4822 (2008).
10. Vajtai, R. Springer Handbook of Nanomaterials. ISBN: 9783642205941 (2013).
11. Nada, H. Importance of water in the control of calcite crystal growth by organic molecules. *Polym. J.* **47**, 84–88 (2015).

12. Hemming, N. G., Reeder, R. J. & Hart, S. R. Growth-step-selective incorporation of boron on the calcite surface, *Geochimica et Cosmochimica Acta*. **62**, 2915–2922 (1998).

13. Folk, R. L. The Natural History of Crystalline Calcium Carbonate: Effect of Magnesium Content and Salinity. *Journal of Sedimentary Petrology* **44**, 40-53 (1974).

14. Davis, K. J., Dove, P. M., Wasylenki, L. E. & De Yoreo, J. J. Morphological consequences of differential Mg^{2+} incorporation at structurally distinct steps on calcite. *Am. Mineral.* **89**, 714–720 (2004).

15. Stephenson, A. E., Hunter, J. L., Han, N., Deyoreo, J. J. & Dove, P. M. Effect of ionic strength on the Mg content of calcite : Toward a physical basis for minor element uptake during step growth. *Geochim. Cosmochim. Acta* **75**, 4340–4350 (2011).

16. Renard, F., Montes-Hernandez, G., Ruiz-Agudo, E. & Putnis, C. V. Selenium incorporation into calcite and its effect on crystal growth: An atomic force microscopy study. *Chem. Geol.* **340**, 151–161 (2013).

17. Orme, C. A. *et al.* Formation of chiral morphologies through selective binding of amino acids to calcite surface steps. *Nature* **411**, 775–779 (2001).

18. Teng, H. H., Dove, P. M., Orme, C. A. & De Yoreo, J. J. Thermodynamics of Calcite Growth : Baseline for Understanding Biomineral Formation. *Science* **282**, 724–727 (1998).

19. Teng, H. H., Dove, P. M. & De Yoreo, J. J. Kinetics of calcite growth: Surface processes and relationships to macroscopic rate laws. *Geochimica et Cosmochimica Acta* 64, 2255-2266 (2000).

20. Hendley, C. T. *et al.* Mechanistic Insights into Diblock Copolymer Nanoparticle-Crystal Interactions Revealed via in Situ Atomic Force Microscopy. *J. Am. Chem. Soc.* **140**,

7936–7945 (2018).

21. Hendley, C. T. In situ atomic force microscopy of growing crystals reveals fundamental mechanisms of crystal growth and incorporation of additives. Ph.D. thesis, Cornell University (2017).

22. Hofmann, S., Voïtchovsky, K., Spijker, P., Schmidt, M. & Stumpf, T. Visualising the molecular alteration of the calcite (104) - Water interface by sodium nitrate. *Sci. Rep.* **6**, 1–11 (2016).

23. Miyata, K. *et al.* Dissolution Processes at Step Edges of Calcite in Water Investigated by High-Speed Frequency Modulation Atomic Force Microscopy and Simulation. *Nano Lett.* **17**, 4083–4089 (2017).

24. Söngen, H. *et al.* Resolving Point Defects in the Hydration Structure of Calcite (10.4) with Three-Dimensional Atomic Force Microscopy. *Phys. Rev. Lett.* **120**, 116101 (2018).

CHAPTER 2

NANOSCALE EFFECTS OF NICKEL CATIONS ON CALCITE GROWTH OBSERVED BY *IN SITU* ATOMIC FORCE MICROSCOPE

2.1 Introduction

Calcite is the most commonly found form of calcium carbonate in nature[1]. Calcite growth in solution is a well-studied yet not fully understood system[2–10]. The growth of calcite is controlled primarily by the supersaturation of the solution. Additives in solution are believed to a major factor influencing the growth rates and morphologies of calcite[2,4,7,11,12]. Among various techniques that have helped researchers understand, both qualitatively and quantitatively, crystal-additive interactions in calcite growth, AFM is widely used[9,10,13,14]. Scientists have succeeded in characterizing *in situ* growth of calcite using AFM and have developed multiple crystallization models to describe calcite growth, including hillock growth and crystal-additive interaction models[2,15–17]. Among the possible types of crystal-additive interaction mechanisms[17], the effect of the kinetic coefficient (β) in the equation describing step velocities (eq. 1.1) is interesting but relatively less studied[2,6,15,17]. In this study, *in situ* AFM is applied to characterize the effect of nickel (II), a cation with an unusual hydration shell, on calcite growth, specifically as it relates to the surface hydration layer of calcite.

AFM studies on calcite give direct insights into how additives interact with calcite. One well-studied calcite-additive system is the Ca-Mg system[4,7,14,18]. Magnesium can substitute for calcium during calcite growth and thus incorporate into the lattice and induce local strains. It changes the thermodynamics of the system (i.e., the K_{sp} is modified) and as a result, modifies the morphology of the calcite and inhibits calcite hillock growth. Other studies, including research on some amino acids, which act as surfactants to modify the surface free energy of calcite[5], and research on step pinners of calcite hillocks, such as abalone shell proteins[15,19,20], all addressed the importance of altering thermodynamics during calcite-additive interactions to achieve modification of the crystals.

In addition to altering the thermodynamics of crystallization with additives, additives can change the kinetic coefficient[10,12,17]. The kinetic coefficient is defined in Equation 1.1 and it gives important information about behaviors of atoms at the calcite surface, including desolvation, diffusion and adsorption. Researchers started to realize the importance of surface kinetics at the beginning of this century. For example, a study on the Ca-Sr system showed an enhancement of calcite growth with a range of Sr concentration, suggesting possible modification of the surface kinetics[10]. Other efforts have focused on systems which are not as complicated as calcite systems, and researchers have reached some preliminary conclusions about kinetic coefficients in different crystal systems[21,22]. However, without a better understanding on surface solvation, the mechanisms by which the impurities affect kinetic coefficient remain unclear.

During recent years, we have gained a deeper understanding of the structure of the water layers on top of calcite surfaces as a result of advances in computation and surface characterization techniques[23–28]. Studies on the calcite surface suggest that a complex hydration layer, composed of two water molecular layers and one possible extra water molecular layer above it, exists when the calcite is exposed to an aqueous solution[23,25,29]. Such a double-layer water interface might account for various properties that calcite has shown in solution growth, including the difference in properties of acute and obtuse steps, and the attachment behaviors of certain molecules. This hydration layer is involved in behaviors related to the kinetic coefficient such as desolvation and adsorption. The water molecules around the kink sites must be displaced to add growth units, and the energy to displace such water layer contributes to the kinetic coefficient term. Thus, if a certain additive is able to modify the energy penalty for displacing the water molecules, the growth kinetics could be changed significantly.

In more recent studies, researchers have explored how additives can disrupt the surface hydration of calcite. Monovalent cations including sodium are added to the growth solution purposefully to modify the ionic strength and disrupt surface hydration[6,30]. Larger molecules including polymers can also control calcite growth by modifying kinetics. A study by the Dove group suggested that hydrophilicity of peptides had major effect on calcite growth kinetics[31] by the impact of negative charges on calcite hydration layer. The growth rate of calcite could be enhanced by addition of oligomeric aspartic acid, which only induced weak electrostatic forces at the step edges, and the rate enhancement was believed to result from an increase in the kinetic coefficient[31]. Such observations suggest the importance of desolvation barriers in the process of incorporation of crystal growth units. For example, evidence has been found that a family of charged peptoids modified calcite growth by disrupting the surface hydration as indicated by changes in kinetic factors[32,33].

Divalent cations possess complex hydration shells in aqueous solution[34–39]. In this work, we are motivated to see how cations with different hydration shells interact with the surface hydration layer of calcite and if we can modify calcite growth by introducing such cations to calcite growth. A magnesium cation has a stable single hydration shell composed of 6 water molecules around the core. The effect of this single hydration shell is not obvious on calcite growth according to previous results. We have chosen to characterize the effect of another divalent cation, nickel, on calcite growth. Nickel is slightly smaller in size than magnesium, while it has two stable hydration layers around the core and a smaller enthalpy of solvation. The aim of this work is to tackle unresolved problems of calcite growth by a focus of surface chemistry: how does the calcite hydration layer affect attachment of growth units, and how does the hydration shell of the added cations, e.g. Ni(II), affect calcite growth. We predict that besides

incorporating into calcite, like what happens in the Ca-Mg system, the nickel cations will have a greater influence on calcite surface chemistry due to its secondary solvation shell (Fig. 2.1). To investigate how such a cation with a double hydration shell interact with calcite during crystallization, we have conducted a series of AFM experiments on Ca-Ni system.

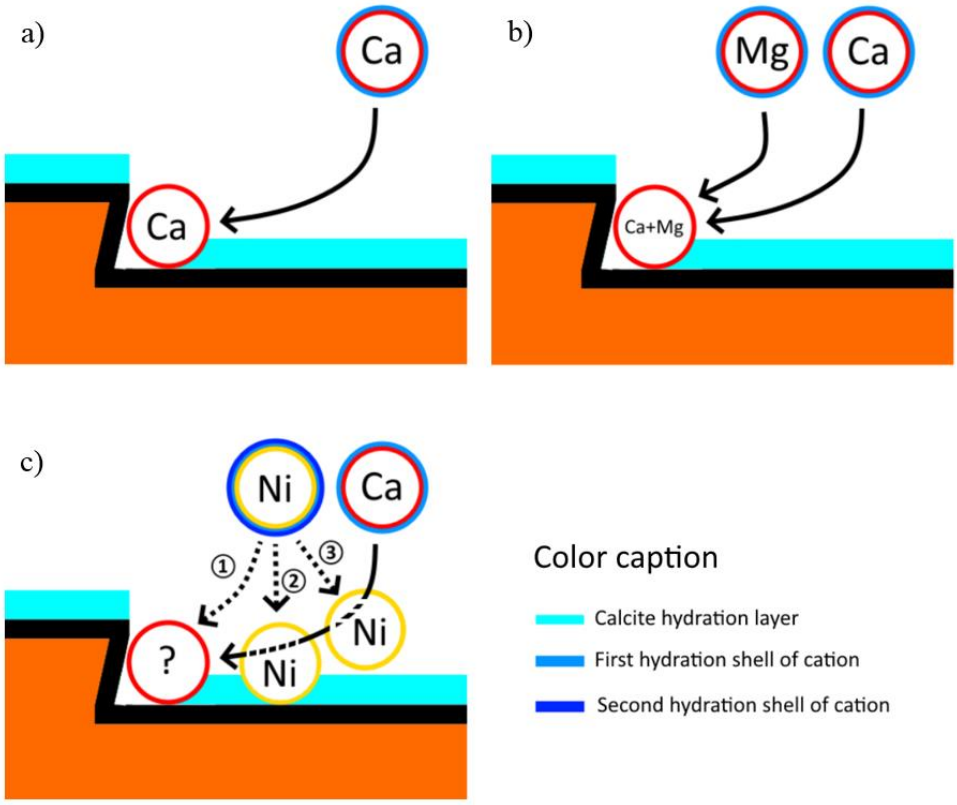

Fig. 2.1 Schematic drawings showing possible attachment mechanisms of divalent ions to the calcite surface during growth. (a) Calcium ions attach to kinks and steps in pure calcite growth solution. The growth rate of calcite is dependent on supersaturation. (b) With magnesium, both Mg cations and Ca cations can attach to the steps. Mg competes with Ca to bond with carbonate, forming magnesium carbonate, which inhibits calcite growth and decreases the step velocity. (c) With nickel, calcite growth may be modified through different pathways. The nickel cations can behave like magnesium and incorporate into the calcite hillock (path ①). The nickel cations can also influence the pathway of calcium attachment. They could either "dive" into the calcite surface hydration layer and disrupt it (path ②), or simply float above the hydration layer (path ③).

2.2 Methods

2.2.1 Atomic force microscopic observation on calcite growth in fluid cell

Geologic calcite single crystals were purchased from Ward's Scientific, and were cleaved to parallelogram-shaped thin pieces with the size of roughly 1.5 cm x 1.5 cm. All pieces were freshly cleaved using chisels and razor blades and a smooth {104} surface of each piece was used for AFM characterization. Nitrogen flow was applied to remove possible particulates before imaging. De-ionized water of resistance 18.2 Mohm was used for all aqueous solutions. A 50 mL solution of 0.018 M $CaCl_2$ (CHEM-IMPEX INT'L INC., 99.84%), a 50 mL solution of 0.0394 M NaCl (BAKER ANALYZED REAGENT, >=99%) and 0.0302 g $NaHCO_3$ (MALLINCKRODT CHEMICALS, >=99%) (0.0036 M) powder were mixed to make 100 mL calcite growth solution. The calcite supersaturation of the growth solution is 1.61 and the pH value was ~8.4 after degassing with nitrogen. For growth solution with nickel additives, the same Ca^{2+} supersaturation and pH value were kept, while $NiCl_2$ (ALDRICH CHEMISTRY, 98%) (0.18 mM, 0.27 mM, 0.36 mM, 0.54 mM, or 1.8 mM) was added to the growth solution. Each 100 mL growth solution was evenly distributed to three clean 60 mL syringes and sealed well with parafilm to prevent degradation in air. A syringe pump controlled solution flow through the fluid cell at 0.3 mL/min at room temperature.

Calcite growth was observed using a Bruker Multi8 ® AFM, operated in contact mode (2 Hz scan rate) with Bruker SNL-10 and DNP-S10 tips (tip information attached in Appendix.3). The syringe was replaced every ~20 minutes to prevent degradation of calcite growth solution. The scanning progress was paused briefly while replacing the syringe to prevent vibration of probes and possible damage to growth hillocks.

2.2.2 Quantitative analysis

Quantitative analysis was conducted using data collected by AFM during calcite growth. Among various observable phenomena by AFM, changes in hillock geometry and step velocity are two major indicators of the calcite-additive interaction mechanism. Quantitative analysis focused on low Ni^{2+} concentration where AFM characterization provided sufficient data for quantitative calculation of step velocities. At low Ni^{2+} concentration, hillock morphology was not obviously modified and thus is not discussed here.

For each AFM image, a single line profile was analyzed at the center of a hillock. The height of the hillock over a 5 μm length was quantified and compared for hillocks present at different time points. Such height profiles in terms of horizontal position provided a direct "side view" of the observed calcite hillock. It also indicated the extent of changes in hillock slope over time after the addition of nickel cations (Fig. 2.2b).

For some measurements, it is useful to have the AFM probe scan a single line rather than a 2-dimensional area. For example, scanning a line across the peak of a hillock can show how the hillock slope changes as a function of time. This type of data can be represented by a plot in which the x-axis is horizontal position information while the y-axis indicates the time scale (Fig. 2.2c). This kind of single-axis scan offers a more intuitive visualization of growth trends of step edges as well as a reliable method for quantitative calculation of step velocity[40]. Step velocities are obtained by calculating the horizontal movement of a single point on the step edge as a function of time (i.e., the slope of the dashed red line in Fig. 2.2c). A representative plot of step velocities of both acute and obtuse steps before and after the addition of nickel is shown in Fig. 2.4d.

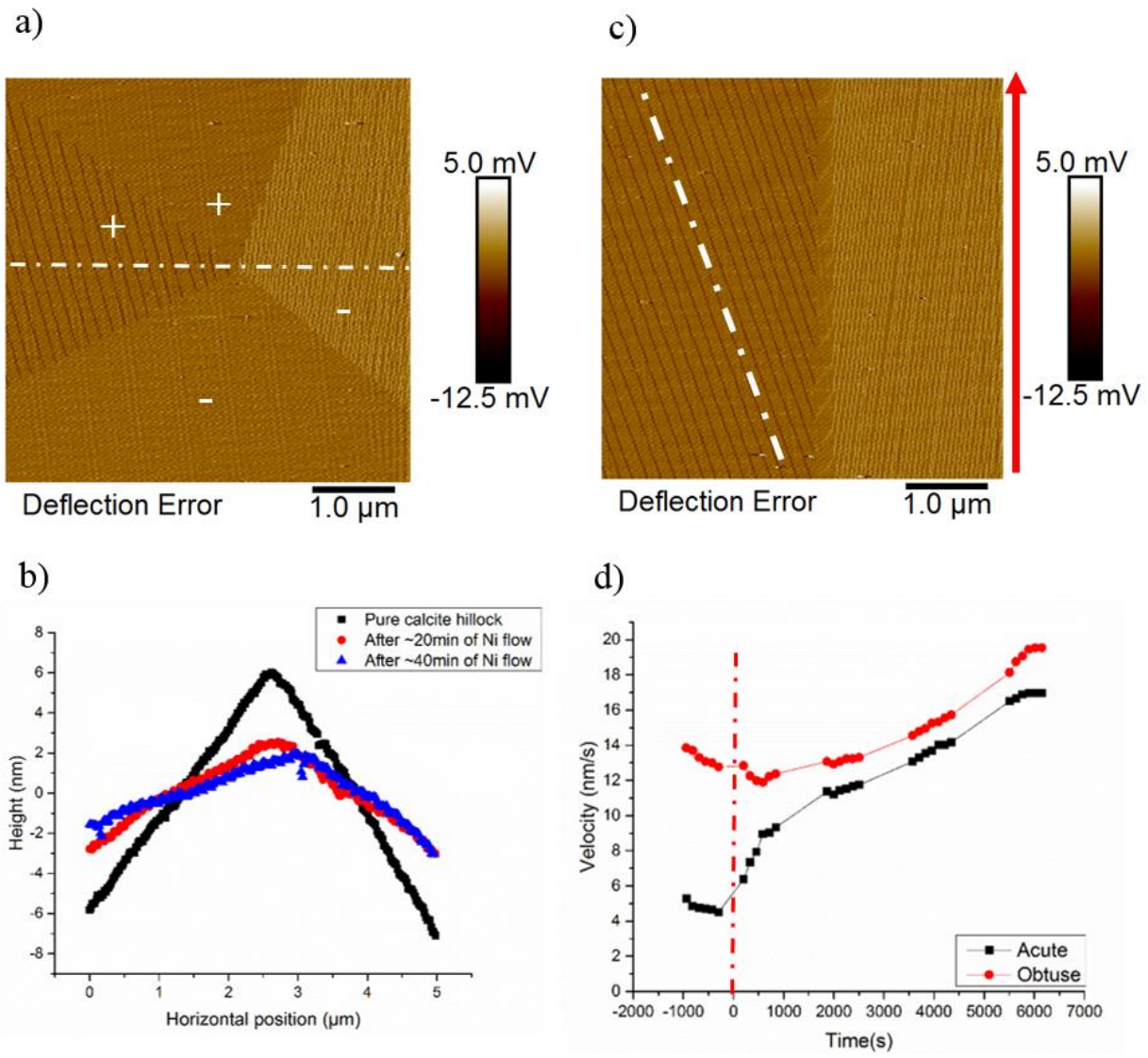

Fig. 2.2 Representative sets of AFM images showing methods of step density and step velocity analysis (a) Step density/ slope analysis is conducted by retrieving height profile of a given line over the hillock peak and (b) "side view" of the hillock can be plotted in term of horizontal position. Three curves of the same peak during one experiment indicates change of step density after addition of nickel. (c) An AFM image of single-axis scan where the AFM tip is fixed to only scan the line indicated in (a). Such single-axis scan integrates the information of the same line over time, giving a direct view of how features (e.g. step edges) change with time. (d) A plot showing step velocity change over time during calcite growth with Ni:Ca = 1.5 mol%. This plot shows a typical trend of step velocity change: the step velocity increases with presence of nickel cations.

2.2.3 Scanning electron microscopic characterization on bulk calcite

Bulk calcite crystal growth was accomplished using the vapor diffusion method[41] (Fig. 2.3). Ammonium carbonate powder and calcium chloride solution were put into two distinct containers sealed with parafilm. Small holes were poked into the parafilm in order to allow carbon dioxide and ammonia gases to diffuse from the sublimation of the ammonium carbonate into the $CaCl_2$ solution, resulting in crystallization of calcium carbonate. A photograph of the setup is shown in Fig. 2.3b. Two glass vials containing 10 mM $CaCl_2$ solution were put in close proximity to the petri dish, which holds 0.5 g $(NH_4)_2CO_3$ powder (ALDRICH CHEMISTRY, 99.99%). $CaCl_2$ hydrate pellets (STERM CHEMICALS, 99.99%) were added as dessicant at the bottom of the dessicator. A silicon wafer was added to each vial as a substrate for crystal nucleation.

Three sets of bulk growth experiments were conducted. The first group of vials without additives is a control group representing pure calcite growth by vapor diffusion. The second group contains 1 mol% Ni^{2+} additive in both vials and the third group contains 3 mol% Ni^{2+} additive in both vials. After 48 hours of vapor diffusion growth, crystals were observed on the silicon wafer substrates. Both wafers were washed with De-ionized water and flushed with nitrogen gas after taken out of the vials. The samples were coated with platinum and were then characterized under Zeiss Gemini scanning electron microscope using the High efficiency secondary electron (HE-SE2) Detector.

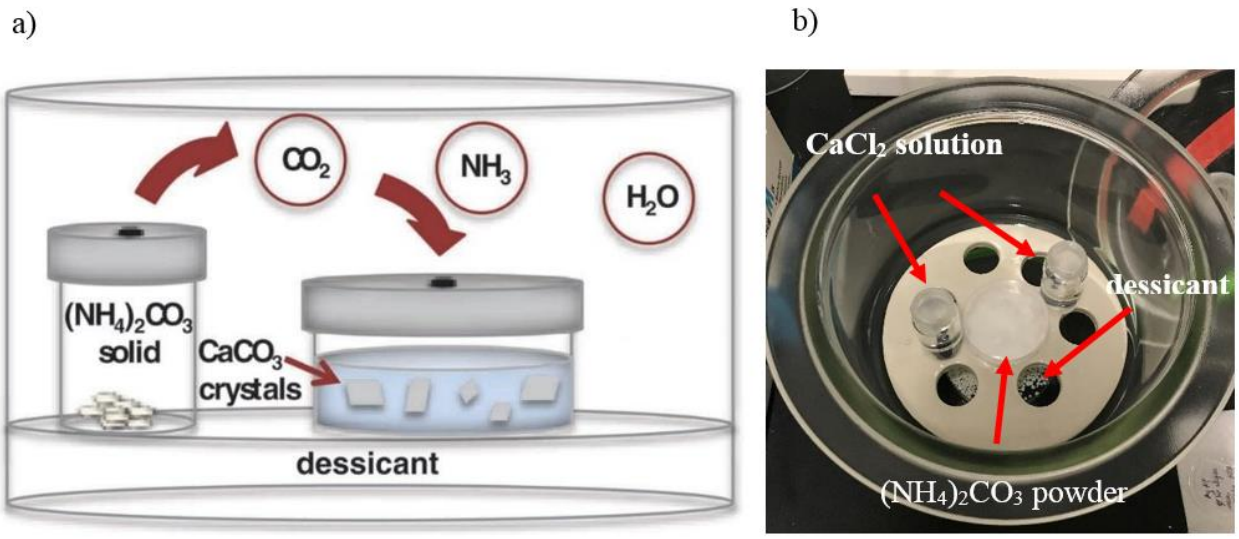

Fig. 2.3 Experimental method for bulk calcite growth with nickel additives. (a) A schematic diagram of a typical single vapor diffusion setup representing how carbon dioxide gas moves into the calcium growth solution and forms calcite crystals. (b) a photo of experimental setup showing details of the dessicator, the location of the glass vials and the petri-dish, and the dessicant. (a) reprinted from ref.41 with permission from WILLEY-VCH copyright 2012.

2.3 Results

2.3.1 Modification of hillock geometry

Spiral hillock growth of calcite was observed on a {104} calcite surface using AFM. Before the addition of Ni^{2+} to the growth solution, the hillocks showed well-defined vicinal faces with two obtuse step-edges (+) and two acute step-edges (-) (Fig. 2.4 a,d,g). The obtuse step edges show a much smaller step density than the acute step edges. The structural difference between acute steps and obtuse steps accounts for different properties of these two step types and preference of impurities to attach on one particular step type[17].

After addition of Ni^{2+} to the growth solution, modification of hillock geometry was observed. Several concentrations of Ni have been studied and three representative conditions are shown in Fig. 2.4. At a lower Ni concentration (<3 mol%), the step density of calcite hillocks decreases significantly after addition of Ni (Fig. 2.4 b,e) and keeps decreasing with time (Fig. 2.4 c,f). The difference between obtuse step density and acute step density has been significantly decreased. After 40 minutes of Ni addition, the obtuse step density and acute step density are almost the same (Fig. 2.4c). The hillock morphology is mostly maintained while minor step rounding effects are observed at the boundary of acute-obtuse steps (Fig. 2.4 c,f). At a higher Ni concentration (3 mol%), strong modification of hillock morphology is observed at the acute steps. Step rounding at acute steps suggests incorporation of nickel cations into the growing calcite hillock. Similar to what happens at lower concentration, the step densities on both acute and obtuse steps decrease significantly with time. An experiment was conducted with 10 mol% Ni additive (see Appendix A.2). After the introduction of this much Ni, the calcite hillock lost its hillock features. Due to this devastating influence on calcite hillocks caused by high concentration of nickel, all further experiments were performed at low nickel concentration (<Ni 3 mol%).

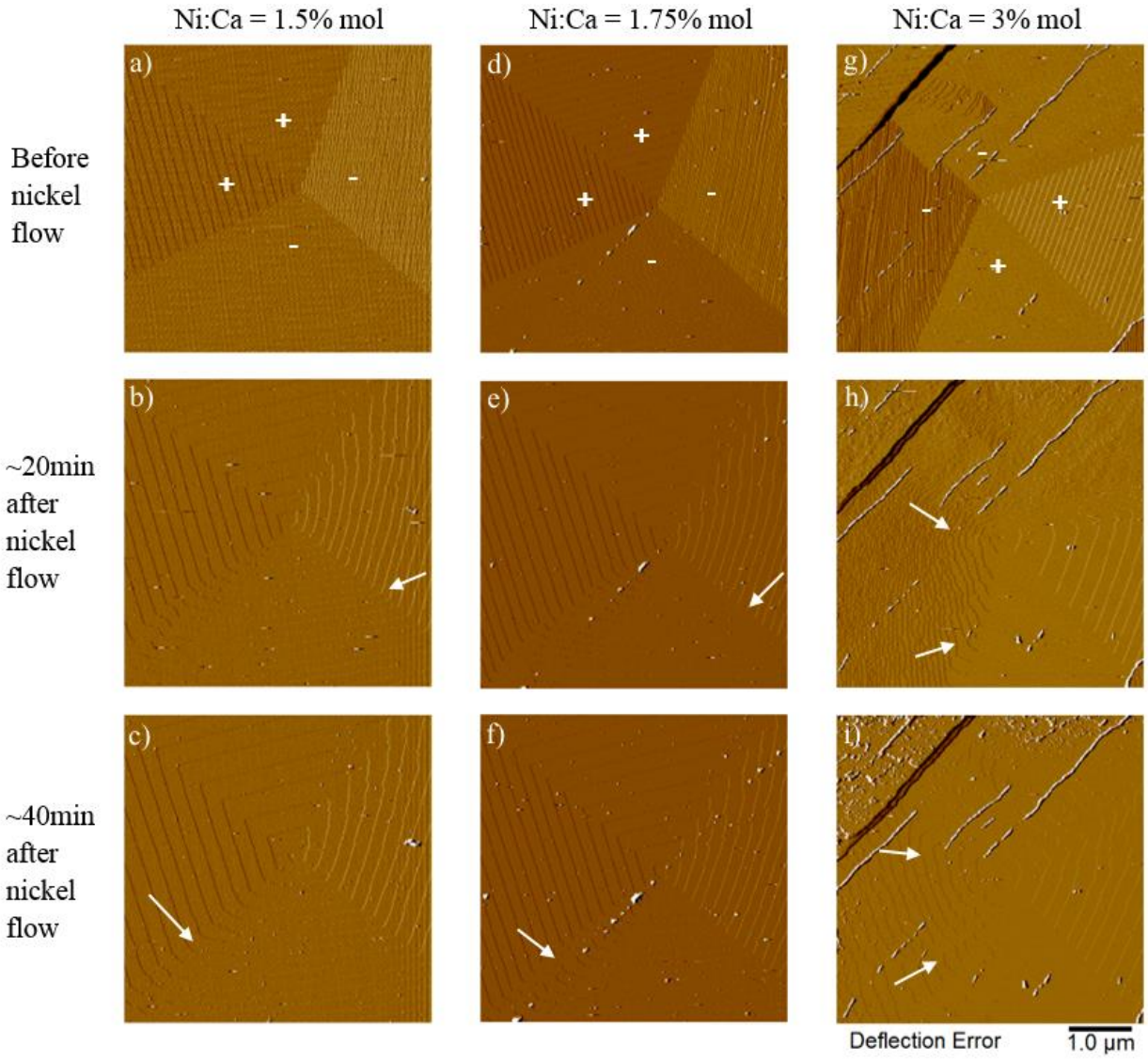

Fig. 2.4 Representative sets of AFM images of calcite hillocks growing with nickel of different concentration. (a-c) Calcite hillock grown with 1.5 mol% Ni. (d-f) Calcite hillock grown with 1.75 mol% Ni. (g-i) Calcite hillock grown with 3 mol% Ni. Images (a)(d)(g) show calcite hillocks before addition of nickel, (b)(e)(h) show the hillocks ~20 minutes after addition of nickel, and (c)(f)(i) show the hillocks ~40 minutes after addition of nickel. Acute and obtuse steps are indicated by "-/-" and "+/+" respectively in (a)(d)(g). Arrows in (c)(f) show minor step rounding at acute-obtuse boundary. Arrows in (h), (i) show major step rounding at acute steps.

2.3.2 Step density quantification

Step density quantification is visualized by the slope of the hillock peaks across a 5 µm area. Calcite hillocks from three different experiments (0.5 mol%, 1 mol% and 1.5 mol% Ni addition experiments) were analyzed and compared (Fig. 2.5). Before addition of nickel, all hillocks had similar peak height (8-12 nm) across a 5 µm area. One of the hillocks was about 3 nm (25%) lower than the other two, which possibly resulted from a neighboring competing hillock causing a lower local supersaturation. About 20 minutes after addition of different concentrations of nickel to the three hillocks, the slope of each hillock decreased significantly. The peak heights across a 5 µm area were all reduced to ~5 nm and such a large change was independent of the nickel concentration. After 20 more minutes, the hillock slope did not change significantly compared to the previous frames. This phenomenon suggested that hillock step density reached a steady state and no longer was changing with time.

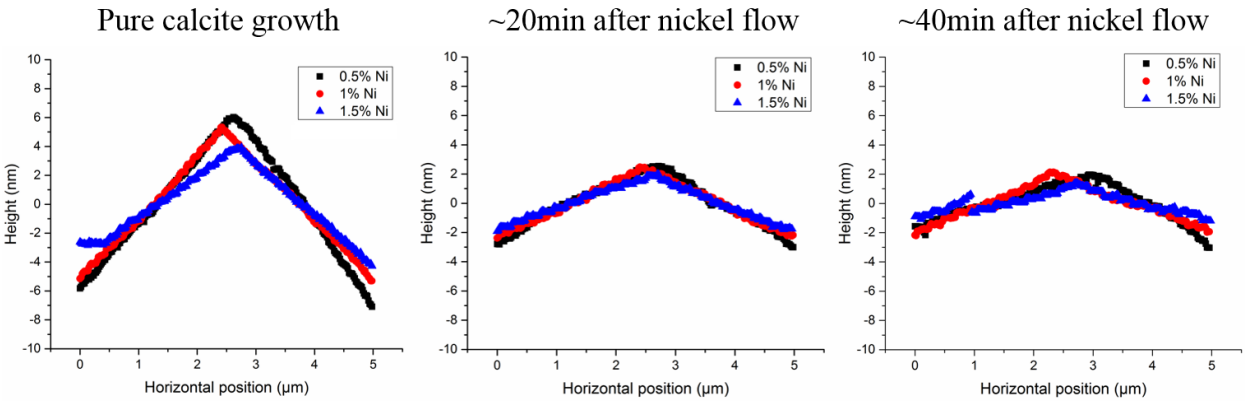

Fig. 2.5 Step density quantification visualized by height of hillock peaks across a 5-um area. (a) Three calcite hillocks growing with pure calcite growth solution. The height of the hillocks over a 5-um area are about 8~12 nm. (b) About 20 minutes after addition of nickel (0.5 mol%, 1 mol% and 1.5 mol% respectively), the slope of each hillock is severely decreased. (c) About 40 minutes after addition of nickel, slope of each hillock is not noticeably changing.

In Fig. 2.5c, the hillock grown with 1.5 mol% Ni (blue curve) shows a chasm at about 1 μm position. Such an atypical hillock feature is believed to result from a neighboring hillock overgrowing this central hillock even though they are supposed to grow under the same supersaturation. Such abnormal overgrowth behavior of hillocks is currently not well-understood and is discussed further in Chapter 3.

2.3.3 Step velocity quantification

Step velocity quantification was conducted with 5 different concentrations of nickel (0.5 mol%, 1 mol% 1.25 mol%, 1.5 mol% and 1.75 mol% Ni addition experiments). A general trend of increasing step velocity is observed for all Ni concentrations and for both acute and obtuse steps (Fig. 2.6). Before the addition of nickel, the step velocities of the acute steps of each hillock were similar (~ 3.5-5.5 nm/s) and these velocities kept stable over about 1000 seconds. The obtuse step velocities varied slightly among experiments: in 3 cases, they were stable at ~10-12 nm/s, while in the other 2 cases, the velocities were ~13-14 nm/s and showed a slightly decreasing trend over about 1000 seconds before the addition of nickel. The values of data are in a reasonable range compared to previous studies of calcite growth[4,7,10]. The fluctuation in velocity may result from competing hillocks around the central hillocks.

After the addition of nickel, the acute step velocities for all five cases increased significantly in the first 1000 seconds. Cases with higher nickel concentration (1.5 mol% and 1.75 mol%) showed a more robust increase in step velocities. According to the trends of collected data, the acute step velocities reached steady state after a certain amount of time. The time taken to reach steady state varied with nickel concentration, but no obvious relationship was observed. In contrast, the obtuse step velocities initially decreased and then started to increase

after about 500 seconds. The trends of the plots also suggest that a steady state may be eventually reached, but the current data sets are not able to track the hillock until the obtuse steps reached the steady state. The overall increasing trends of the velocities of both the acute and obtuse steps were the same.

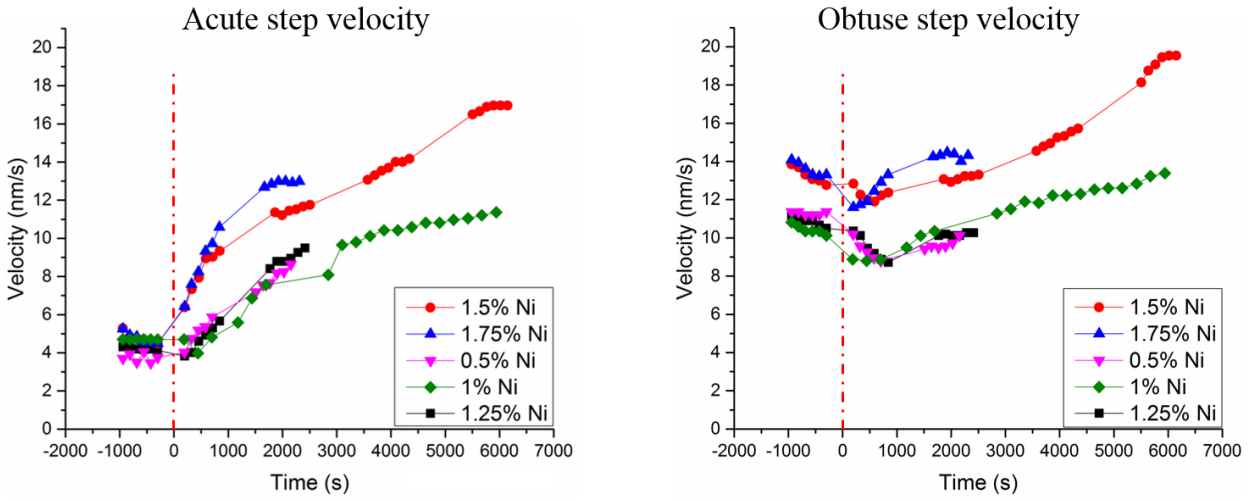

Fig. 2.6 Step velocity quantification using single-axis scan. The data includes five cases with different nickel concentration varying from 0.5% to 1.75%. (a) Acute step velocities increase significantly with presence of nickel. The velocities increase in about 1500 seconds after addition of nickel, and slowly increase afterwards until they possibly reach a steady state after a long time (~6000 seconds). (b) Obtuse step velocities first decrease with addition of nickel until about 500 seconds and then start to increase. The step velocities increase to different extents with respect to different nickel concentration.

2.3.4 Expansion of surface defects

Addition of nickel to calcite growth solutions modifies both geometry and step velocity of calcite hillocks. Besides these most representative phenomena, the presence of nickel also induces abnormal expansion of surface defects. After the addition of nickel, an obvious trend of expansion was observed on both large defects and minor defects (Fig. 2.7). Such a trend was observed regardless of nickel concentration. The sizes of surface scratches on both hillocks (Fig. 2.7 a,c) were enlarged. On step edges of the hillocks, surface defects became observable several

minutes after introduction of nickel to the growth solution. The longer the hillocks were exposed to nickel, the higher the density of surface defects visible in one frame. There is a clear preference for formation of defects on the acute steps over obtuse steps (Fig. 2.7 b,d).

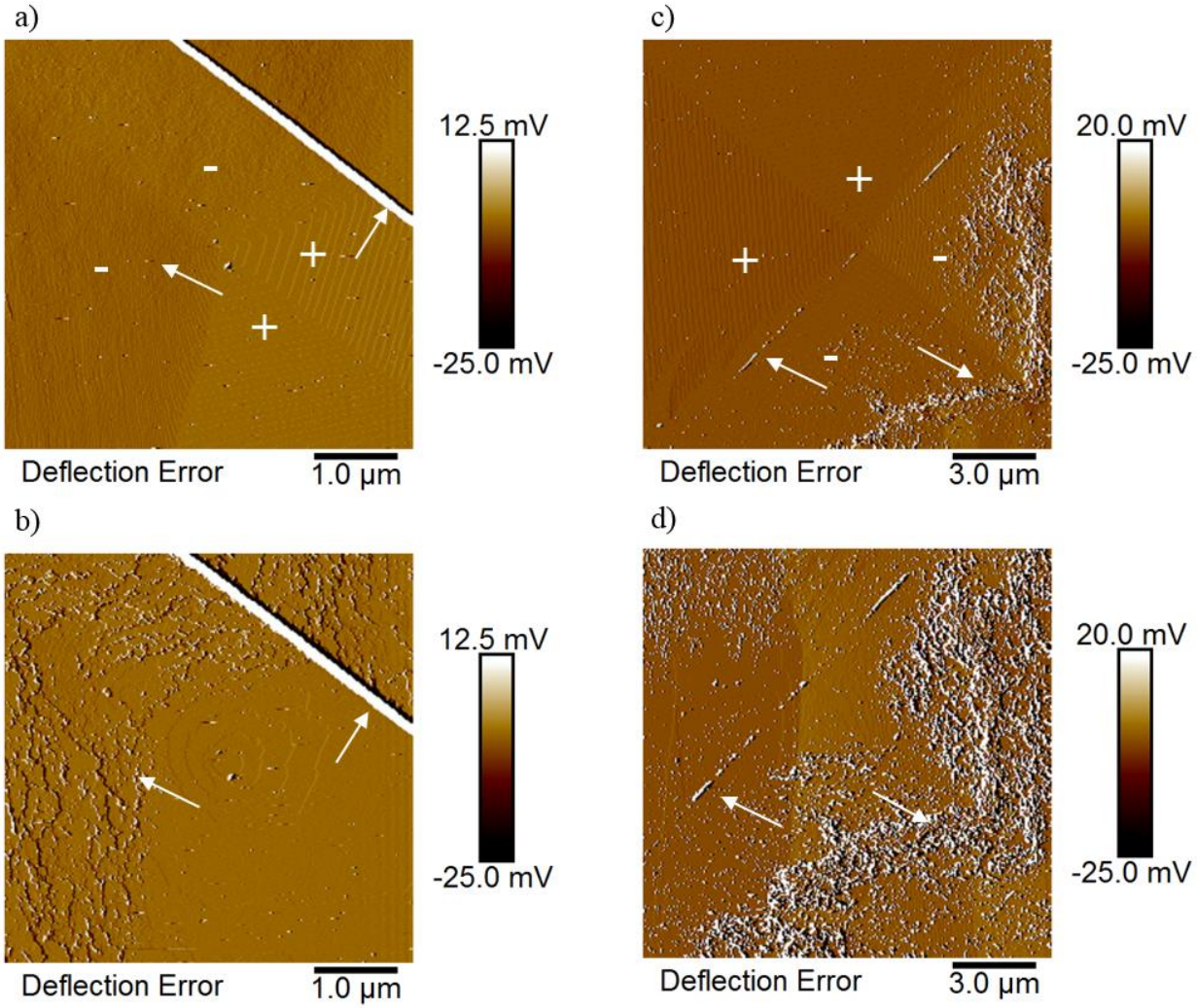

Fig. 2.7 A representative set of AFM images of calcite hillocks showing expansion of surface defects after addition of nickel. (a, b) After addition of 3% Ni, defect sites expand significantly at acute steps. The scan area is 5 µm x 5 µm. (c, d) In a separate experiment, after addition of 1.75% Ni, defects expand significantly on acute steps. Since this sample has more pre-existing defects, such behavior is more obvious, and expansion of defects are also observed at obtuse steps. The scan area is 15 µm x 15 µm. Arrows indicate expansion of pre-existing, observable scratches, as well as additional surface defects that grow with time.

2.3.5 Bulk calcite crystal characterization

Calcite-additive interaction can be also observed on bulk calcite crystals grown with different concentrations of the additive. The crystal shape, especially the preferably indicated facet(s), gives important insight into how additives effect calcite growth[4,5,17,40,42]. Bulk crystal growth was conducted using the single vapor diffusion method for pure calcite and two nickel concentrations (1 mol% and 3 mol% Ni). The SEM images shown in Fig. 2.8 show representative single crystals grown in these conditions.

Control calcite crystals grown under pure growth solution showed a consistent rhombohedral shape (Fig. 2.8a). Calcite crystals grown with 1 mol% Ni generally maintained rhombohedral morphologies (Fig. 2.8b). However, some degree of flaws was detected at the edges and corners. Gaps were observed at the edges and the corners were not fully grown. The same trend was observed for calcite crystals grown with 3 mol% Ni, with even more obvious changes to the edges and corners (Fig. 2.8c). The {104} facets remained smooth, while the corners and edges appeared rough and incomplete. These roughened "facets" approximately correspond to {001} and {018} facets.

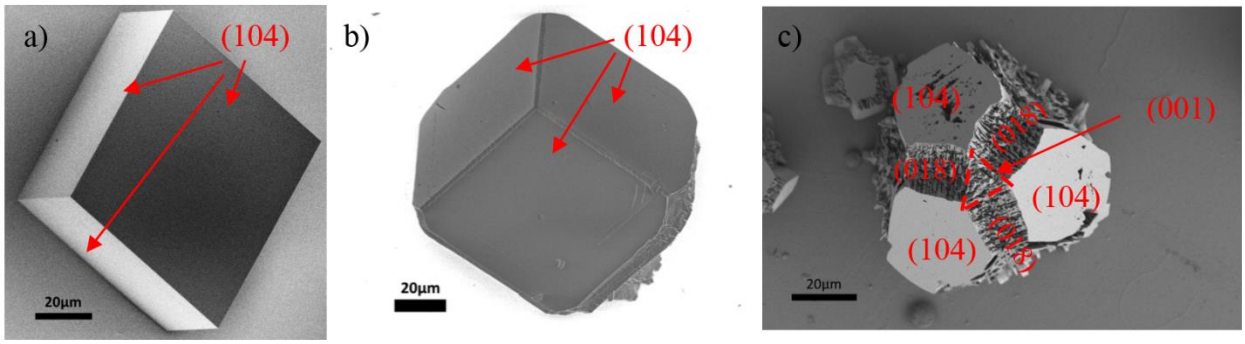

Fig. 2.8 A representative set of SEM images of bulk crystal growth using 5mM $CaCl_2$ and vapor diffusion of carbon dioxide. (a) Calcite grown with pure growth solution. (b) Calcite grown with 1 mol% Ni addition. (c) Calcite grown with 3 mol% Ni addition.

2.4 Discussion

Addition of nickel to calcite growth solutions induced large changes to hillock geometry an bulk crystal morphology. At higher Ni concentration (3 mol%), the nickel cations behaved similarly to magnesium cations[7,14], where they incorporate to calcite hillocks and hindered calcite growth, as indicated by step rounding observed by AFM. The step rounding was much more obvious on acute steps than obtuse steps, implying that the nickel is more likely to incorporate into acute steps. Consistent with the AFM observations, we observed that the bulk crystal shape remained rhombohedral in general, but the edges were rough compared to bulk calcite grown under pure condition. The large amount of surface defects observed on bulk crystals also were consistent with the AFM experiments in which nickel promoted the generation and expansion of surface defects.

Unlike the hillocks at high Ni concentrations, the hillocks and bulk crystals grown at lower Ni concentrations (< 3 mol%) showed only little modification on the morphology. Even though the morphology remained constant, we observed significant changes in both the step densities and step velocities at these lower Ni concentrations. First, there was an obvious decrease in step density, indicating that either the effective supersaturation ($a_{Ca^{2+}} - a_{Ca^{2+}eq}$) was decreased or the surface free energy γ was increased as a result of the addition of Ni to the system. Considering the large extent of step density decrease, it is unlikely that the surface free energy alone was increased, since a large change in surface free energy should induce obvious morphology change similar to the cases of amino acid additives[5]. Thus, the alternative explanation for the change in step density, a decrease in effective supersaturation is more likely to occur as a result of nickel in the solution. We hypothesize that at low Ni concentration, nickel cations thermodynamically influence calcite growth by decreasing the driving force for

crystallization. Such decrease is possibly accomplished by a decrease in local solubility of calcite induced by incorporation of a certain amount of nickel. The lack of significant step rounding, however, suggests only minor incorporation behaviors of nickel at low concentration. One possible explanation is that nickel carbonate has a much larger solubility product, *Ksp* (1.42 E-7), than that of calcium carbonate (3.36 E-9)[43]. If a small amount of $NiCO_3$ causes the *Ksp* of calcium carbonate to increase and thus increases the equilibrium activity of calcium $a_{Ca^{2+}eq}$, it eventually leads to a decrease in effective supersaturation. Further measurements of step density and step velocities as a function of calcium concentration would be required to confirm the source of such change in thermodynamics[4,14].

The step velocity analysis showed that addition of nickel enhanced hillock growth, since both obtuse and acute step velocities increased with the addition of nickel (Fig. 2.6). Since step velocity is determined by two variables, the effective supersaturation and the kinetic coefficient, β (Equation 1.1), an increase in step velocity and a decrease in effective supersaturation indicates that the kinetic coefficient, β, must be increased to compensate for the decrease in effective supersaturation. Such a change in the kinetic coefficient suggests a large disruption of the pathway through which the growth units go and attach on the crystal substrate[31]. The nickel cations can go through path #2 shown in Fig 2.1, where they go into the surface hydration layer of calcite and disrupt the water molecule distributions, making the growth units easier to attach on calcite surface. Since the increase in acute velocity was significant, we assume that the local hydration layer on the acute steps is disrupted by the presence of nickel, allowing more facile addition of calcite growth units to the acute steps. The nickel cations can also interact with the hydration layer by path #3, where they stay above the hydration layer and do not disrupt the distribution of water molecules, causing only trivial influence on surface hydration. Since we

observed a large change in the kinetic coefficient, nickel cations are less likely to interact with the hydration layer by path #3, however, no decisive evidence has proven either of the mechanisms.

Besides an increasing trend of step velocities, the step velocity graphs showed more detailed information. A decrease in obtuse step velocities was observed during the first few seconds after addition of nickel. Such a decrease possibly corresponds to the significant increase in acute step velocity. Since growth on the acute steps are preferred by nickel adsorption, more growth units attach at acute steps. The rapid increase of growth units attaching to acute steps will change the local equilibrium condition, affecting the neighboring steps, especially the parts close to the (+/-) boundaries. After a certain amount of time, such a sudden change can be 'buffered' by the overall aqueous environment, where the supersaturation of calcite can support robust growth at both kinds of steps. Eventually, the effect of fluctuations on the local equilibrium was compensated for and the obtuse step velocities start to increase similar to the acute step velocities. Noticeably, step velocities kept increasing for a long time before some of the trials (1% and 1.5% Ni) reached steady state. However, we could not achieve steady state for all trials even though we continued some trials to ~ 2 hours. There are two possible explanations for such a phenomenon. The more probable case is that the effect of nickel cations is limited by diffusivity[7]. Since we kept the flow rate constant for both pure calcite growth solution and nickel-added growth solution, it was possible that the diffusivity of the cations was changed after introduction of nickel and became the limiting factor of the reaction. The second assumption is that the presence of nickel cations in the solution forms complexes with other ions, shifting the chemical condition to a much more complex case[44]. Calcite growth can possibly become a self-catalyzing process after introduction of nickel, which causes the step velocity to increase

continuously for a long time. Neither hypothesis could be proven based on the current data sets. Changing the flow rate of each experiment can help us understand how diffusivity limits the crystallization process with presence of nickel. In addition, an even longer trial that allows us to see the arrival of steady state or computational simulations may help find the reason for the timely increasing velocities.

Expansion of surface defects and the "torn" shape of bulk calcite crystal grown with 3% Ni may also suggest a shift in preference of growth unit attachment. During pure calcite growth, large surface defects, such as scratches and large holes detectable by AFM (size > AFM tip diameter), usually remain unchanged while minor surface defects are usually covered due to calcite growth. However, both observable large defects and minor defects expand during growth with nickel. Particularly on acute steps, existing defects kept expanding and new defects kept appearing independent of Ni concentration. Such phenomenon cannot be fully explained according to current knowledge, but we hypothesize that local dissolution is happening around the defects. Since the calcite hillock was growing at a much faster rate, it is possible that calcite dissolves at the unfavorable attachment sites such as defects, and is transported to more favorable sites such as acute steps. This hypothesis cannot be proven at this time, but it is consistent with observations in bulk calcite growth. The calcite grown in the presence of 3 mol% Ni showed the possible development of an unfavorable {001} facet, which is consistent with our AFM characterizations on calcite growth with high concentration Ni. The obtuse steps were rounded at high Ni concentration while the surface defects grew on both acute and obtuse edges, which resulted in the roughened {001} and {018} facets[45]. For the bulk crystals, we can assume that the three hillocks representing each of the {104} facets all have severely rounded acute steps with a high density of surface defects. This results in an incomplete {001} facet and crystal

edges with large density of surface defects. Large surface defects were also observed more frequently on calcite grown with nickel addition. The bulk calcites grown with nickel provided us with preliminary insights into controlling crystal growth using divalent cations like nickel. A comprehensive study on calcite growth and its relationship to pre-existing and newly introduced surface defects might help understand the mechanism and how addition of divalent cations can influence such mechanism.

2.5 Conclusion

We characterized the growth of calcite, including step velocities, hillock step densities, and bulk crystal morphologies, in the presence of nickel cation additives. Our results using different Ni concentrations suggest a concentration-dependent interaction mechanism between nickel and calcite. At higher nickel concentrations, nickel behaves like magnesium, where the divalent cations incorporate into the calcite hillocks and hinder calcite growth. At lower nickel concentrations, though nickel cations reduce thermodynamic driving force for crystallization, it kinetically enhances crystal growth, which result in overall faster step velocities. Such change in kinetic factor is hypothesized to be a result of surface hydration disruption. We believe that disruption on surface kinetics results from disruption of hydration layer by nickel cations due to the large double-layer hydration shell surrounding one nickel cation while in aqueous solution, and evidence of their temporary presence on calcite surface instead of other attachment behaviors such as incorporation and pinning. Our SEM characterization of bulk calcites are consistent with the AFM findings, especially for the expansion of surface defects induced by addition of nickel, suggesting a possible method of calcite crystallization control. These results

provide insight into how small cations with large hydration shells can lead to unexpected changes to calcite growth kinetics, which may provide a route to modify the hydration layer on crystal surface and thus further influence the interaction between crystal and organic impurities.

Further experiments, such as hydration lateral force study[46], are required to collect more decisive evidence of hydration layer interactions. Computational simulations might also help us better understand the calcite-nickel interaction mechanism and how nickel causes expansion of surface defects. Overall, this work provides us with insight on how to disrupt the surface hydration layer of calcite to achieve significant modification on calcite crystal growth, which in turn could be applied to tune the interaction between calcite and other additives.

2.6 Reference

1. Addadi, L. & Weiner, S. Biomineralization: Mineral formation by organisms. *Phys. Scr.* **89**, (2014).
2. Nielsen, L. C., De Yoreo, J. J. & DePaolo, D. J. General model for calcite growth kinetics in the presence of impurity ions. *Geochim. Cosmochim. Acta* **115**, 100–114 (2013).
3. Kim, Y. Y. *et al.* Tuning hardness in calcite by incorporation of amino acids. *Nat. Mater.* **15**, 903–910 (2016).
4. Davis, K. J., Dove, P. M., Wasylenki, L. E. & De Yoreo, J. J. Morphological consequences of differential Mg^{2+} incorporation at structurally distinct steps on calcite. *Am. Mineral.* **89**, 714–720 (2004).
5. Orme, C. A. *et al.* Formation of chiral morphologies through selective binding of amino acids to calcite surface steps. *Nature* **411**, 775–779 (2001).
6. Hendley, C. T. *et al.* Mechanistic Insights into Diblock Copolymer Nanoparticle-Crystal Interactions Revealed via in Situ Atomic Force Microscopy. *J. Am. Chem. Soc.* **140**, 7936–7945 (2018).
7. Davis, K. J., Dove, P. M. & De Yoreo, J. J. Resolving the Control of Magnesium on Calcite Growth: Thermodynamic and Kinetic Consequences of Impurity Incorporation for Biominernal Formation. *Mat. Res. Soc. Symp.* **620**, 1–7 (2000).
8. Hemming, N. G., Reeder, R. J. & Hart, S. R. Growth-step-selective incorporation of boron on the calcite surface, *Geochimica et Cosmochimica Acta*. **62**, 2915–2922 (1998).
9. Renard, F., Montes-Hernandez, G., Ruiz-Agudo, E. & Putnis, C. V. Selenium incorporation into calcite and its effect on crystal growth: An atomic force microscopy study. *Chem. Geol.* **340**, 151–161 (2013).

10. Wasylenki, L. E., Dove, P. M., Wilson, D. S. & De Yoreo, J. J. Nanoscale effects of strontium on calcite growth: An in situ AFM study in the absence of vital effects. *Geochim. Cosmochim. Acta* **69**, 3017–3027 (2005).

11. Meyer, H. J. The influence of impurities on the growth rate of calcite. *J. Cryst. Growth* **66**, 639–646 (1984).

12. Lin, Y. P., Singer, P. C. & Aiken, G. R. Inhibition of calcite precipitation by natural organic material: Kinetics, mechanism, and thermodynamics. *Environ. Sci. Technol.* **39**, 6420–6428 (2005).

13. Chow, E. H. H., Bučar, D. K. & Jones, W. New opportunities in crystal engineering - The role of atomic force microscopy in studies of molecular crystals. *Chem. Commun.* **48**, 9210–9226 (2012).

14. Davis, K. J. Magnesium as an impurity in calcite growth: Thermodynamic and kinetic controls on biomineral formation. Master thesis, Georgia Institute of Technology (2000).

15. Kubota, N. & Mullin, J. W. A kinetic model for crystal growth from aqueous solution in the presence of impurity. *J. Cryst. Growth* **152**, 203–208 (1995).

16. Andersson, M. P. *et al.* A Microkinetic Model of Calcite Step Growth. *Angew. Chemie - Int. Ed.* **55**, 11086–11090 (2016).

17. Qiu, S. R. & Orme, C. A. Dynamics of biomineral formation at the near-molecular level. *Chem. Rev.* **108**, 4784–4822 (2008).

18. Stephenson, A. E., Hunter, J. L., Han, N., De Yoreo, J. J. & Dove, P. M. Effect of ionic strength on the Mg content of calcite: Toward a physical basis for minor element uptake during step growth. *Geochim. Cosmochim. Acta* **75**, 4340–4350 (2011).

19. Lutsko, J. F. *et al.* Crystal growth cessation revisited: The physical basis of step pinning.

Cryst. Growth Des. **14**, 6129–6134 (2014).

20. Walters, D. *et al*. Modification of calcite crystal growth by abalone shell proteins: an atomic force microscope study. *Biophys. J.* **72,** 1425 (1997).

21. Land, T. A., De Yoreo, J. J. & Lee, J. D. An in-situ AFM investigation of canavalin crystallization kinetics. *Surf. Sci.* **384**, 136-155 (1997).

22. Vekilov, P. G. & Rosenberger, F. Dependence of lysozyme growth kinetics on step sources and impurities. *J. Cryst. Growth* **158**, 540-551 (1996).

23. De La Pierre, M., Raiteri, P. & Gale, J. D. Structure and Dynamics of Water at Step Edges on the Calcite {1014} Surface. *Cryst. Growth Des.* **16**, 5907–5914 (2016).

24. Dorvee, J. R. & Veis, A. Water in the formation of biogenic minerals: Peeling away the hydration layers. *J. Struct. Biol.* **183**, 278–303 (2013).

25. Söngen, H. *et al.* Resolving Point Defects in the Hydration Structure of Calcite (10.4) with Three-Dimensional Atomic Force Microscopy. *Phys. Rev. Lett.* **120**, 116101 (2018).

26. Miyata, K. *et al.* Dissolution Processes at Step Edges of Calcite in Water Investigated by High-Speed Frequency Modulation Atomic Force Microscopy and Simulation. *Nano Lett.* **17**, 4083–4089 (2017).

27. Hofmann, S., Voïtchovsky, K., Spijker, P., Schmidt, M. & Stumpf, T. Visualising the molecular alteration of the calcite (104) - Water interface by sodium nitrate. *Sci. Rep.* **6**, 1–11 (2016).

28. Marutschke, C. *et al.* Three-dimensional hydration layer mapping on the (10.4) surface of calcite using amplitude modulation atomic force microscopy. *Nanotechnology* **25**, (2014).

29. Perry IV, T. D., Cygan, R. T. & Mitchell, R. Molecular models of a hydrated calcite mineral surface. *Geochim. Cosmochim. Acta* **71**, 5876–5887 (2007).

30. Stephenson, A. E., Hunter, J. L., Han, N., De Yoreo, J. J. & Dove, P. M. Effect of ionic strength on the Mg content of calcite : Toward a physical basis for minor element uptake during step growth. *Geochim. Cosmochim. Acta* **75**, 4340–4350 (2011).

31. Elhadj, S., De Yoreo, J. J., Hoyer, J. R. & Dove, P. M. Role of molecular charge and hydrophilicity in regulating the kinetics of crystal growth. *Proc. Natl. Acad. Sci.* **103**, 19237–19242 (2006).

32. Chen, C. L., Qi, J., Tao, J., Zuckermann, R. N. & De Yoreo, J. J. Tuning calcite morphology and growth acceleration by a rational design of highly stable protein-mimetics. *Sci. Rep.* **4**, 1–11 (2014).

33. Chen, C. L., Qi, J., Zuckermann, R. N. & De Yoreo, J. J. Engineered biomimetic polymers as tunable agents for controlling $CaCO_3$ mineralization. *J. Am. Chem. Soc.* **133**, 5214–5217 (2011).

34. Hamm, L. M., Wallace, A. F. & Dove, P. M. Molecular dynamics of cation hydration in the presence of carboxylated molecules: Implications for calcification. *Mater. Res. Soc. Symp. Proc.* **1301**, 51–61 (2011).

35. Waluyo, I. *et al.* The structure of water in the hydration shell of cations from x-ray Raman and small angle x-ray scattering measurements. *J. Chem. Phys.* **134**, (2011).

36. Liu, H. Y. *et al.* Characterizing Ni(II) hydration in aqueous solution using DFT and EXAFS. *J. Mol. Model.* **22**, 1–9 (2016).

37. Egorov, A. V., Komolkin, A. V., Lyubartsev, A. P. & Laaksonen, A. First and second hydration shell of Ni^{2+} studied by molecular dynamics simulations. *Theor. Chem. Acc.* **115**, 170–176 (2006).

38. Wheeler, O. W., Carl, D. R. & Armentrout, P. B. Second–shell thermochemistry for

hydration of strontium dications as determined by threshold collision-induced dissociation and computations. *Int. J. Mass Spectrom.* **429**, 76–89 (2018).

39. Rodriguez-Cruz, S. E., Jockusch, R. A. & Williams, E. R. Hydration energies of divalent metal ions, $Ca^{2+}(H2O)_n$ (N = 5-7) and $Ni^{2+}(H2O)_m$ (N = 6-8), obtained by blackbody infrared radiative dissociation. *J. Am. Chem. Soc.* **120**, 5842–5843 (1998).

40. Teng, H. H., Dove, P. M. & De Yoreo, J. J. Kinetics of calcite growth: Surface processes and relationships to macroscopic rate laws. *Geochimica et Cosmochimica Acta* 64, 2255-2266 (2000).

41. Asenath-Smith, E., Li, H., Keene, E. C., Seh, Z. W. & Estroff, L. A. Crystal growth of calcium carbonate in hydrogels as a model of biomineralization. *Adv. Funct. Mater.* **22**, 2891–2914 (2012).

42. Ihli, J. *et al*. Visualization of the effect of additives on the nanostructures of individual bio-inspired calcite crystals. *Chem. Sci.* **10**, 1176-1185 (2019)

43. Lide, D. R. CRC handbook of chemistry and physics : a ready-reference book of chemical and physical data 87th edition. ISBN: 9780849304873 (2006).

44. Sebastiani, F. et al. Water Dynamics from THz Spectroscopy Reveal the Locus of a Liquid–Liquid Binodal Limit in Aqueous $CaCO_3$ Solutions. *Angew. Chem. Int. Ed.* **56**, 490 –495 (2017).

45. Smeets, P. J. M. et al. A Mesocrystal-Like Morphology Formed by Classical Polymer-Mediated Crystal Growth. *Adv. Funct. Mater.* **27**, 1701658 (2017).

46. Diao, Y. & Espinosa-Marzal, R. M. Effect of Fluid Chemistry on the Interfacial Composition, Adhesion and Frictional Response of Calcite Single Crystals – Implications for Injection-Induced Seismicity. *J. Geophys. Res. Solid Earth* **124**, (2019).

CHAPTER 3

INDICATION OF DISRUPTION ON CALCITE HYDRATION LAYER BY NICKEL CATIONS: CONCLUSIONS AND FUTURE WORKS

3.1 Conclusions

The aim of this project was to tackle an unresolved question in calcite growth by focusing on surface chemistry: how does the calcite hydration layer effect attachment of growth units, and how does the hydration shell of added cations effect calcite growth? In this thesis work, I used in situ AFM to observe calcite growth in the presence of different nickel concentrations. I studied the modification of hillock geometry, change in step velocity, and change of other surface patterns. I also observed bulk calcite growth with nickel impurities using SEM.

Based upon my data, we conclude that the nickel cations effect calcite growth by changing surface kinetics, consistent with a of disruption of the calcite surface hydration layer. We compared calcite hillocks growing with different concentrations of nickel and observed that only a large amount of nickel added to the growth solution would incorporate into calcite surface and cause hillock morphology change. Such observations narrowed our target concentrations, and I performed quantitative analysis using small concentrations of nickel varying from 0.5% to 1.75%. By calculating hillock slope, I found that addition of nickel decreases step density, which is an indication of decreasing effective supersaturation. By studying step velocities of calcite hillock growth for continuous spans (>40 minutes for each experiment), I found that the overall trend of step velocity increased with addition of nickel. I also found different trends on acute and obtuse steps. The acute steps velocities increased immediately after addition of nickel and such an increase was significant. In contrast, the obtuse step velocities decreased at the beginning, while they increased after a certain amount of time and the amount increased was much smaller than that of acute steps. The increasing trend of step velocity combined with a decrease in effective supersaturation indicated a large increase in kinetic coefficient, which represented disruption on surface kinetics after addition of nickel. We believe that disruption on surface

kinetics results from disruption of hydration layer by nickel cations due to the large double-layer hydration shell surrounding one nickel cation while in aqueous solution, and evidence of their temporary presence on calcite surface instead of other attachment behaviors such as incorporation and pinning. The geometry of calcite hillocks can be recovered by removing nickel from growth solution, indicating temporary attachment of nickel on calcite hillocks.

The calcite surface was also modified such that surface defects, especially those on acute steps, were expanded. It suggested an abnormal mechanism by which the nickel cations are affecting the attachment of calcite growth units on calcite surface. We assume that the unusual behavior of the defects is caused by a shift of preferred sites where the growth units attach, while most growth units attach on step edges and calcite dissolves at unfavored sites such as surface defects. Similar modification of preferred growth sites can be observed on bulk calcite crystals grown by vapor diffusion method as well. SEM characterization taught us that {104} facets were not significantly influenced by nickel, except frequently observed surface defects. Meanwhile, {001} and {018} facets were affected largely such that they were not fully indicated compared to the {104} facets.

Nickel-calcite system has very complex interaction mechanisms, and disruption of calcite surface hydration layer is believed to be only one of them. The underlying chemical processes, including nickel cations exchanging water molecules with its surroundings as well as calcite hydration layers, were not completely understood. To thoroughly understand the complex interactions among nickel cations, calcite growth units, and water molecules, more detailed analysis including application of computational models should be conducted in future work in order to explain some experimental results.

3.2 Insight from calcite-polymer-nickel interactions

I also conducted preliminary AFM experiments on calcite growth with nickel as well as large organic particles, which provides some insight to how nickel's hydration shell effects surface kinetics. Several experiments were done with poly(methacrylic acid)-stabilized poly(benzyl methacrylate) nanoparticles ($PMAA_{85}$-$PBzMA_{100}$). This anionic di-block co-polymer forms spherical, micelle structures in aqueous solution and can modify calcite hillock morphology (Fig.3.1.b). The attachment mechanism of this organic particle was described in Dr. Hendley IV's thesis research work[1]. Since the attachment of this organic particle is largely affected by surface chemistry, it is believed to be a promising indicator of how nickel would affect calcite surface water layer.

My preliminary results showed that the attachment mechanism of these organic particles was changed by addition of nickel. The particles attached on the calcite surface and the behavior was consistent with previous findings (Fig. 3.1c)[1]. After addition of nickel, the particles continued to incorporate or hover on calcite surface, however, a trend of particles gathering at step edges were observed (shown by arrows in Fig.3.1, c,d). Height profile showed that the global maximum in height in one frame was still the hillock peak, while local maximum in height appeared at every step, meaning that the large particles were gathering exactly at the step edges. We assume that such behavior is also one result of disruption of surface hydration layer, but further experiments are needed to fully explain this abnormal attachment behavior.

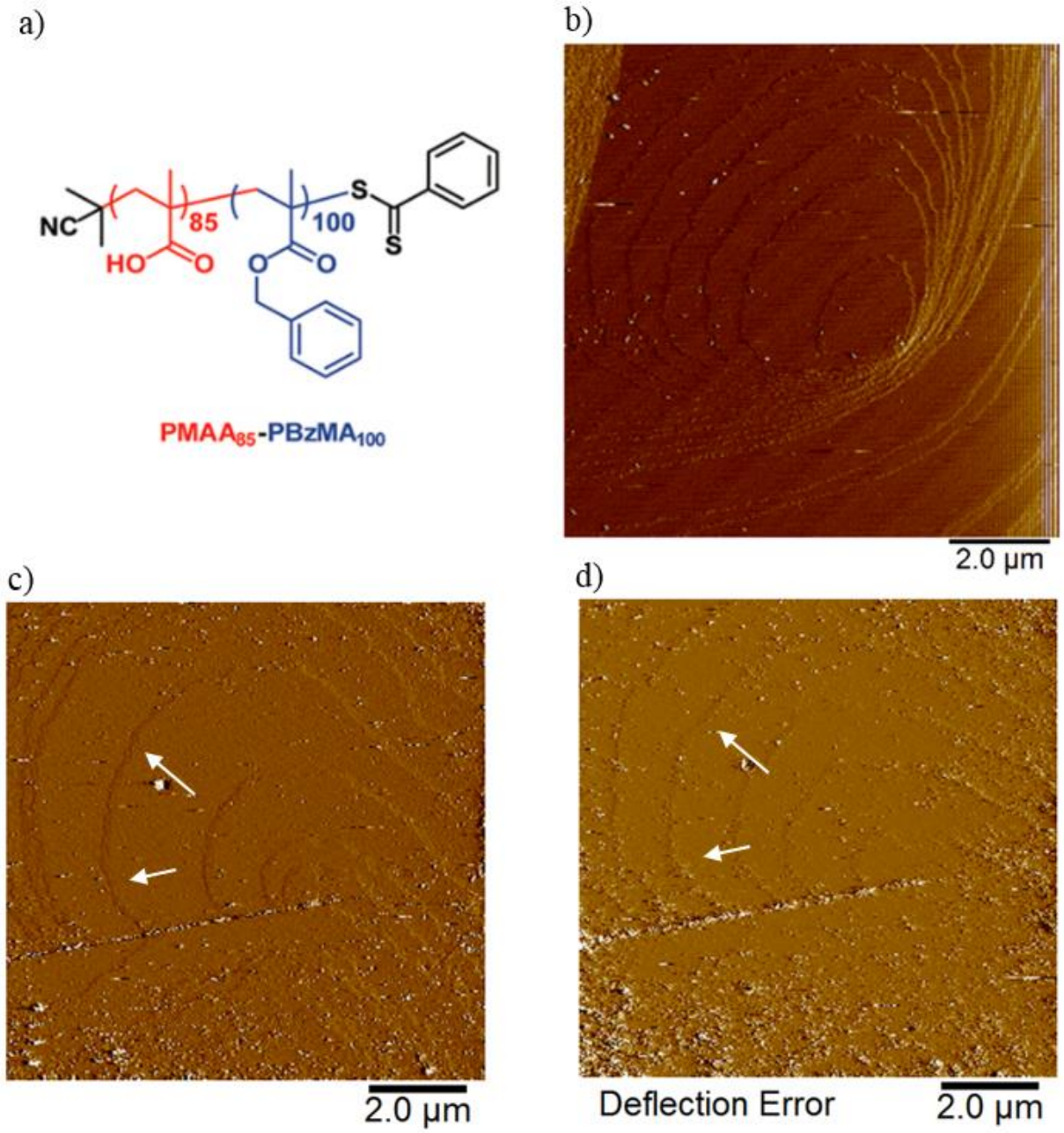

Fig. 3.1 (a) Molecular structure of $PMAA_{85}$-$PBzMA_{100}$ (1). (b) A representative AFM image of calcite hillocks growing with this di-block co-polymer. (c) Before addition of nickel to a calcite hillock growing with $PMAA_{85}$-$PBzMA_{100}$ (d) After addition of nickel to a calcite hillock growing with $PMAA_{85}$-$PBzMA_{100}$. The arrows point to steps where a comparison of local height can be seen. After addition of nickel, the steps became higher than surrounded terraces, indicating gathering of organic particles at the steps. Tapping mode (1.5 Hz scan rate) using Bruker ScanAsyst Fluid+ probes was used to image organic nanoparticles on the calcite surface. (a) reprinted from ref.1 with permission from ACS copyright 2018.

3.3 Future works

To collect more decisive evidence of how nickel cations affect calcite surface hydration, several more experiments can be done in the future. According to our capability, we are able to complete the AFM characterization of calcite hillocks growing with both $PMAA_{85}$-$PBzMA_{100}$ and nickel inclusions. Statistical study on attachment of this organic particle can give us insight on how nickel affects the surface chemistry. We can also conduct inductively coupled plasma studies on bulk calcite crystals to confirm the amount of nickel incorporated into calcite. Both methods can provide firmer evidence on how nickel affects calcite surface chemistry.

To directly study the hydration layer on calcite surface and how cations affect it, we can conduct lateral force AFM studies on a static calcite surface[2]. The specially modeled AFM tips are able to detect lateral force induced by hydration layer when they scan over a calcite surface. By comparing the results for pure water solution and for nickel-included solution, we can tell what extent the nickel cations affect surface hydration[2]. More ideally, researchers may directly observe the calcite hydration layer in atomic resolution using the most advanced AFM techniques in the world[3,4]. Combining computer simulation methods and ultra-high-resolution AFM characterization, future researchers might be able to build a well-established model on how nickel disrupts calcite surface hydration.

In conclusion, this thesis work has built a solid base for better understanding calcite-nickel interaction. More generally, this thesis has explored crystal-additive interaction in a focus of surface chemistry. Hopefully, this thesis work can invoke further research interest on liquid phase crystal growth, and how impurities affect crystallization, which eventually help human to fully understand the mysterious yet charming process of biomineralization.

3.4 References

1. Hendley, C. T. *et al.* Mechanistic Insights into Diblock Copolymer Nanoparticle-Crystal Interactions Revealed via in Situ Atomic Force Microscopy. *J. Am. Chem. Soc.* **140**, 7936–7945 (2018).
2. Diao, Y. & Espinosa-Marzal, R. M. Effect of Fluid Chemistry on the Interfacial Composition, Adhesion and Frictional Response of Calcite Single Crystals – Implications for Injection-Induced Seismicity. *J. Geophys. Res. Solid Earth* **124**, (2019).
3. Miyata, K. *et al.* Dissolution Processes at Step Edges of Calcite in Water Investigated by High-Speed Frequency Modulation Atomic Force Microscopy and Simulation. *Nano Lett.* **17**, 4083–4089 (2017).
4. Söngen, H. *et al.* Resolving Point Defects in the Hydration Structure of Calcite (10.4) with Three-Dimensional Atomic Force Microscopy. *Phys. Rev. Lett.* **120**, 116101 (2018).

Appendix

A.1 Control of pH value for calcite growth experiments

Crystallization of calcite is very sensitive to the pH value of its environment. To control the pH value of every calcite growth experiment, I conducted de-gassing process for every growth solution I made, where I flowed nitrogen gas into the growth solution to decrease the portion of dissolved carbon dioxide. I measured the pH value of several growth solutions and the data is shown in Fig. A.1. The de-gassing process secured a reasonable pH value of each trial (Exp# 4 and Exp# 5). We also see that addition of 3 mol% nickel does not cause a large fluctuation in the pH value of the growth solution (Exp# 6~9).

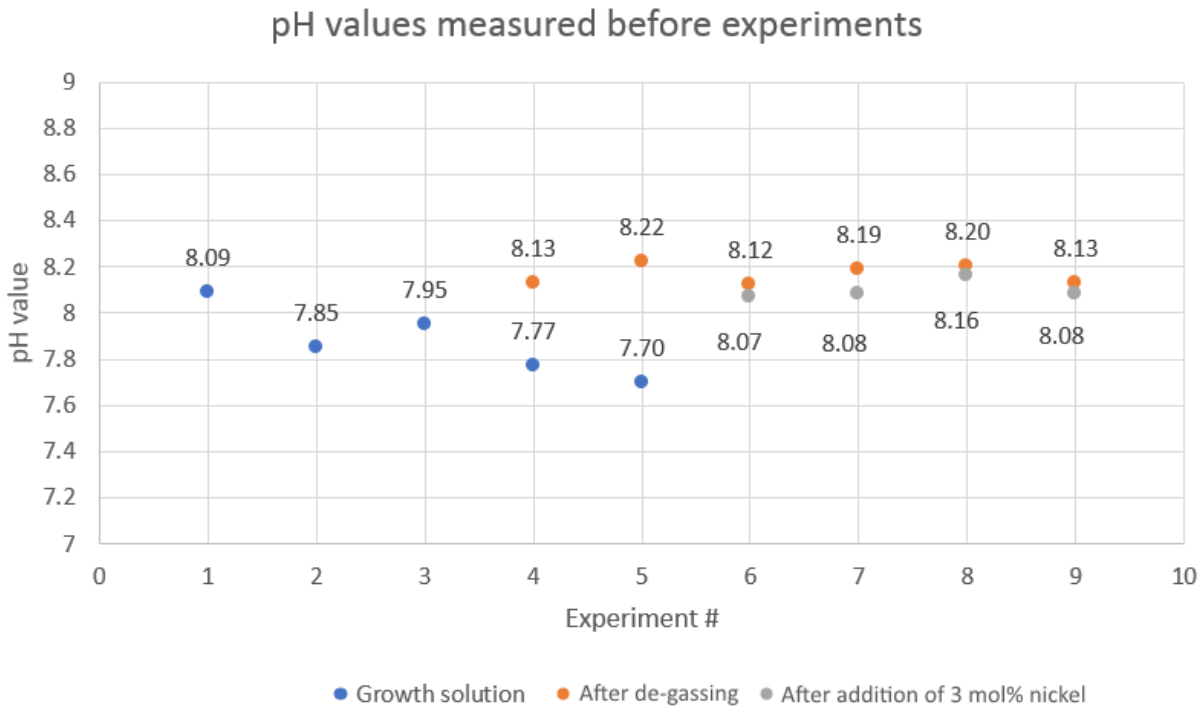

Fig. A.1 A diagram showing control of pH value during calcite growth experiments. De-gassing before conducting calcite growth experiments under AFM is an effective way of removing dissolved carbon dioxide (#4 and #5). Addition of nickel only caused minor changes the pH value of the solution (#6 ~ #9)

A.2 Calcite growth with presence of 10 mol% nickel

Among the AFM experiments I have done on characterizing calcite growth with presence of nickel, one experiment was done with 10 mol% nickel. The calcite growth hillocks dissolved, and step edges became no longer obvious only in 5 minutes after nickel was added. We can assume that such a high concentration of nickel should be decreased largely in order to see slower modification of calcite hillocks. We eventually narrowed our range to 0.5 mol% ~ 3 mol%.

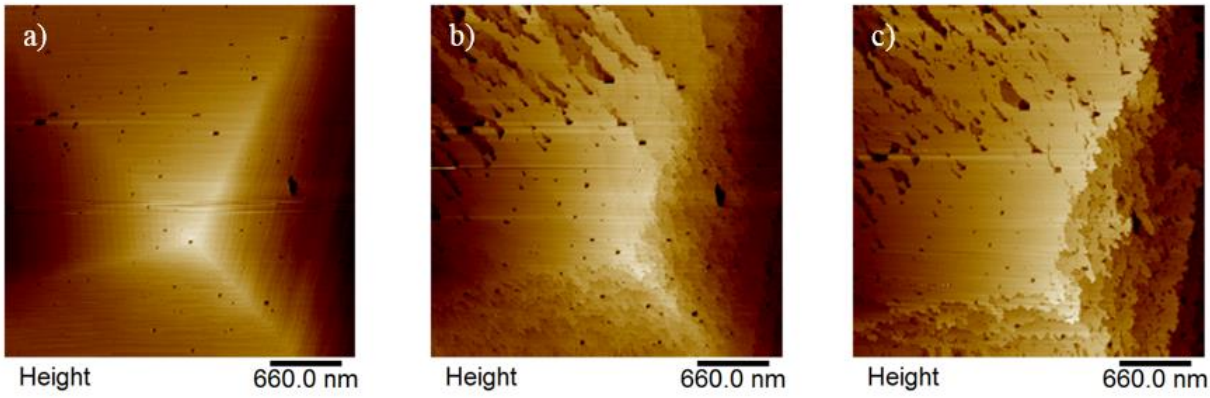

Fig. A.2 AFM images of a calcite hillock growing with 10 mol% nickel addition. (a) The calcite hillock before addition of nickel. (b) The hillock 5 minutes after presence of nickel. (c) The hillock 10 minutes after presence of nickel.

A.3 AFM contact mode tip information

Information about tip geometry is shown below. All parameters of the tips are reproduced from Bruker AFM Probes sales website: https://www.brukerafmprobes.com/.

a)

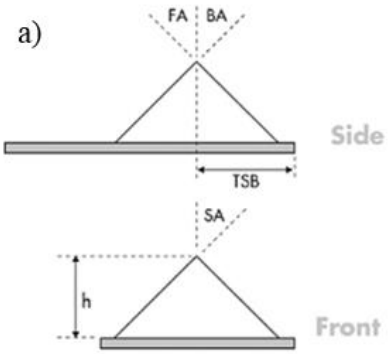

b)

Geometry:	Rotated (Symmetric)
Tip Height (h):	2.5 - 8.0µm
Front Angle (FA):	15 ± 2.5°
Back Angle (BA):	25 ± 2.5 °
Side Angle (SA):	17.5 ± 2.5 °
Tip Radius (Nom):	10 nm
Tip Radius (Max):	40 nm
Tip SetBack (TSB)(Nom):	4 µm
Tip Set Back (TSB)(RNG):	0 - 7 µm

c)

Geometry:	Rotated (Symmetric)
Tip Height (h):	2.5 - 8.0µm
Front Angle (FA):	15 ± 2.5°
Back Angle (BA):	25 ± 2.5 °
Side Angle (SA):	22.5 ± 2.5 °
Tip Radius (Nom):	2 nm
Tip Radius (Max):	12 nm
Tip SetBack (TSB)(Nom):	4 µm
Tip Set Back (TSB)(RNG):	0 - 7 µm

Fig. A.3 Information on tips used in AFM characterization. (a) A schematic drawing of a tip geometry. (b) Information about DNP-S10 tip. (c) Information about SNL-10 tip.